Suction Caissons: Seafloor Characterization for Deepwater Foundation Systems

By

Shadi S. Najjar, Graduate Research Assistant
Robert B. Gilbert, P.E., Ph.D.

Geotechnical Engineering Center
Civil Engineering Department
The University of Texas at Austin

Final Report on the Suction Caissons: Seafloor Characterization for Deepwater Foundation Systems Study
for the Project
Suction Caissons and Vertically Loaded Anchors

Prepared for the Minerals Management Service
Under the MMS/OTRC Cooperative Research Agreement
1435-01-99-CA-31003
Task Order 16169
1435-01-04-CA-35515
Task Order 35980
MMS Project Number 362

and

OTRC Industry Consortium

June 2006

For more information contact:

Offshore Technology Research Center
Texas A&M University
1200 Mariner Drive
College Station, Texas 77845-3400
(979) 845-6000

or

Offshore Technology Research Center
The University of Texas at Austin
1 University Station C3700
Austin, Texas 78712-0318
(512) 471-6989

A National Science Foundation Graduated Engineering Research Center

PREFACE

The project Suction Caissons and Vertically Loaded Anchors was conducted as series of inter-related studies. The individual studies are as follows:

- Suction Caissons & Vertically Loaded Anchors: Design Analysis Methods by Charles Aubeny and Don Murff, Principal Investigators
- Suction Caissons: Model Tests by Roy Olson, Alan Rauch and Robert Gilbert, Principal Investigators
- Suction Caissons: Seafloor Characterization for Deepwater Foundation Systems by Robert Gilbert Principal Investigator
- Suction Caissons: Finite Element Modeling by John Tassoulas Principal Investigator

This report summarizes the results of the Suction Caissons: Seafloor Characterization for Deepwater Foundation Systems, study.

TABLE OF CONTENTS

LIST OF TABLES

LIST OF FIGURES

Introduction

The challenge of seafloor characterization for deepwater facilities is that the mooring foundations, subsea well trees and flowlines are spread over large areas (tens of thousands of feet across), while the cost of obtaining high-quality geotechnical data for the seafloor is high. Therefore, information from a handful of soil borings is typically extrapolated over thousands of feet to design foundations. This extrapolation leads to uncertainty that could potentially lead to excessively conservative designs or to unreliable designs.

The objective of this research was to develop a reliability-based methodology to design suction caisson foundations with typical seafloor characterization data and to apply this methodology to optimize geotechnical investigation programs. The following tasks were completed in order to meet this objective:

1. Quantify effect of spatial variability in soil properties on design for suction caissons.
2. Calibrate and quantify uncertainty in design method for suction caissons.
3. Develop a reliability-based design methodology for suction caissons.
4. Quantify the added value of site characterization data and foundation installation information in reducing uncertainty in suction caisson design.

This research utilized and synthesized the results from a handful of related OTRC projects, including:

- Suction Caisson Model Testing by Olson, Rauch and Gilbert;
- Suction Caisson Predictive Modeling by Aubeny and Murff;
- Suction Caisson Finite Element Modeling by Tassoulas;
- Suction Caisson State-of-Practice by Murff (and API); and
- Mooring System Reliability by Zhang and Gilbert.

Spatial Variability in Suction Caisson Design Parameters

An important issue in site characterization for suction caissons is the spatial variability in geotechnical properties. This variability leads to uncertainty in extrapolating information from boring locations to the actual location of the foundation elements.

Proprietary site investigation and design information was compiled and analyzed for a set of deepwater sites. These data were supplied by three different operators. A database was developed to store and manipulate the data. The design of this database is presented in Appendix A. A database like this, populated with the geotechnical data that is publicly available and submitted to MMS, would be a valuable tool for MMS in evaluating new developments and requalifications.

The data in the database were then analyzed to quantify the spatial variability in design parameters. Figure 1 provides an illustration of results from this work. The data on Figure 1 correspond to boring sites that are in a similar geologic setting, normally consolidated clays from deepwater in the Gulf of Mexico. While similar in geology, these sites are separated by distances ranging from hundreds of feet to hundreds of miles. The design axial capacity was calculated at each boring location for a 60-foot long, 12-foot diameter suction caisson.

Summary statistics for the spatial variability in both axial and lateral caisson capacity are provided in Tables 1 and 2. For comparison purposes, a set of sites from the North Sea, which have a different geologic setting, are also included. Major conclusions from Tables 1 and 2 are: (1) the magnitude of spatial variability in the capacity of suction caissons depends significantly on the geologic setting; and (2) the variability is relatively small for sites with normally consolidated marine clays in deepwater Gulf of Mexico, with coefficients of variation between 0.1 and 0.2.

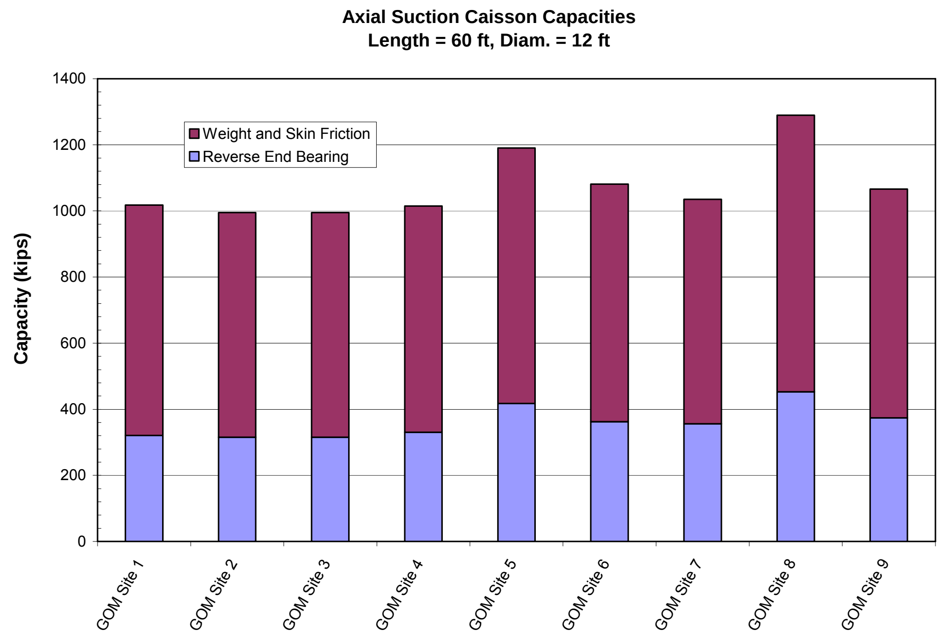

Figure 1. Example of spatial variability in suction caisson capacity across Gulf of Mexico deepwater boring sites.

Table 1. Summary statistics for spatial variability in total axial uplift capacity.

	Length = 60 ft, Diameter = 12 ft		
	Sample Mean (kips)	**Sample Standard Deviation (kips)**	**c. o. v.**
GoM Sites	1076	100	0.09
North Sea Sites	1852	637	0.34
All Sites	1464	596	0.41
	Length = 80 ft, Diameter = 10 ft		
	Sample Mean (kips)	**Sample Standard Deviation (kips)**	**c. o. v.**
GoM Sites	1373	230	0.17
North Sea Sites	2174	517	0.24
All Sites	1773	566	0.32

Table 2. Statistics relating to maximum lateral capacity.

	Length = 60 ft, Diameter = 12 ft		
	Sample Mean (kips)	**Sample Standard Deviation (kips)**	**c. o. v.**
GoM Sites	2021	206	0.10
North Sea Sites	3921	1582	0.40
All Sites	2971	1467	0.49
	Length = 80 ft, Diameter = 10 ft		
	Sample Mean (kips)	**Sample Standard Deviation (kips)**	**c. o. v.**
GoM Sites	3052	430	0.14
North Sea Sites	5533	1582	0.29
All Sites	4293	1467	0.34

In order to better understand the spatial variability in suction caisson capacity, a detailed simulation analysis was conducted (Gilbert and Murff 2001). For comparison purposes, a typical driven steel pipe pile was also included in the analysis since this is the conventional offshore foundation type for shallow water structures (Fig. 2). A generic soil profile for a normally consolidated clay with an undrained shear strength increasing at 10 psf/ft was used to simulate the variability in soil profiles that might exist across a field (Fig. 3). A model presented in Smith and Gilbert (2001), which was calibrated with data from one offshore field, was used to simulate this variability. Twenty-five soil profiles were simulated; an example profile is shown on Fig. 4. The capacities for the generic foundations were then calculated for each simulated profile using conventional design practice (e.g., API 1993).

The results from this analysis are presented in Tables 3, 4 and 5. For axial side shear (Table 3), the effect of variability in shear strength along the length of the pile is more significant for a suction caisson than for a driven pile due to the effect of averaging. Variations in strength tend to average along the length of the pile; intervals with lower than average strength tend to be compensated by intervals with higher than average strength. The longer the pile, the greater the effect of this averaging and the less variability there is in the total skin friction. For axial end bearing, there is significantly greater variability in end bearing than skin friction for both suction caissons and driven piles (Table 4). The variability is greater for end bearing than skin friction because the vertical extent of soil involved in the failure mechanism is smaller and there is less averaging. Since end bearing contributes more to the total axial capacity for a suction caisson than for a driven pile, variations in soil properties will have a greater effect on the estimated end bearing for a suction caisson than for a driven pile. The total added effects of side shear and end bearing are presented in Table 5. Note that there is substantially more variability for a suction caisson that is loaded to failure in a pure lateral versus a pure axial mode. This result occurs because a smaller region of shear effectively contributes to the lateral capacity and there is less averaging than for the axial capacity.

In summary, uncertainties in soil properties will have a relatively greater effect on the estimated axial capacity for a suction caisson compared to a driven pile, and they will have a relatively greater effect on the lateral capacity than on the estimated axial capacity for a suction caisson.

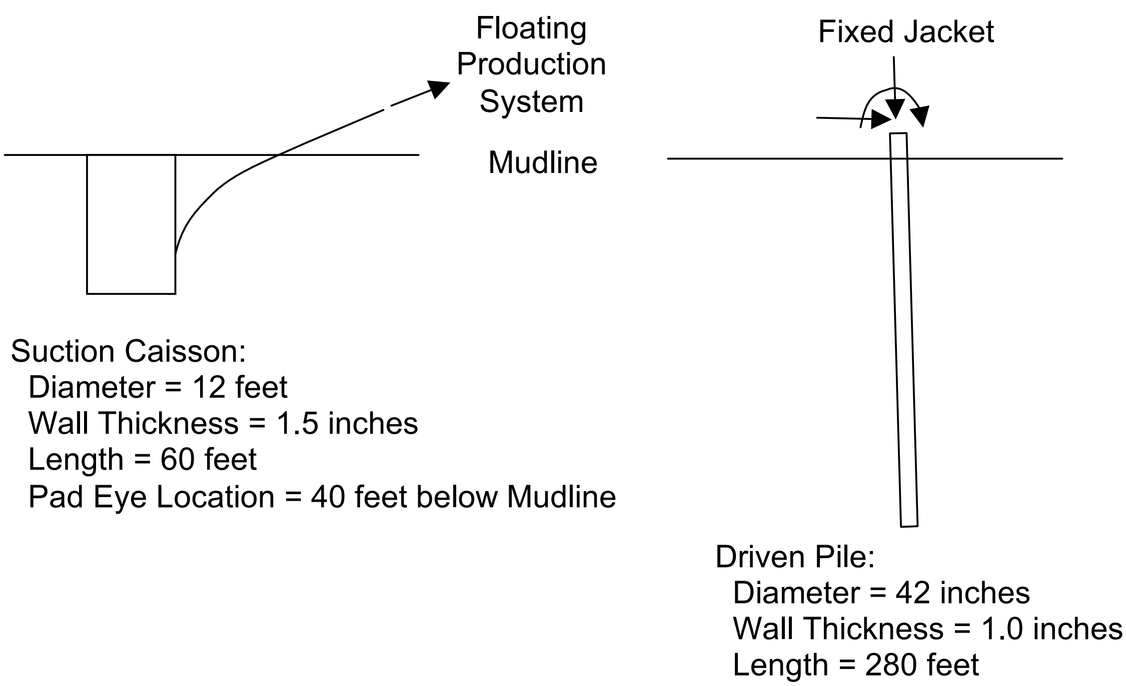

Figure 2. Schematic of generic suction caisson and driven pile.

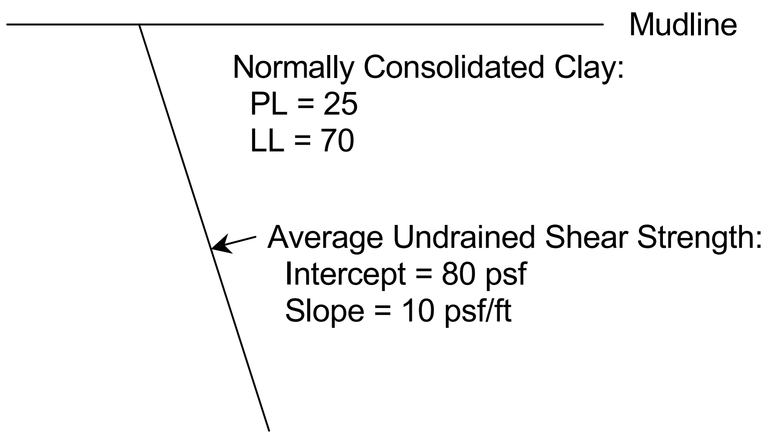

Figure 3. Generic soil profile.

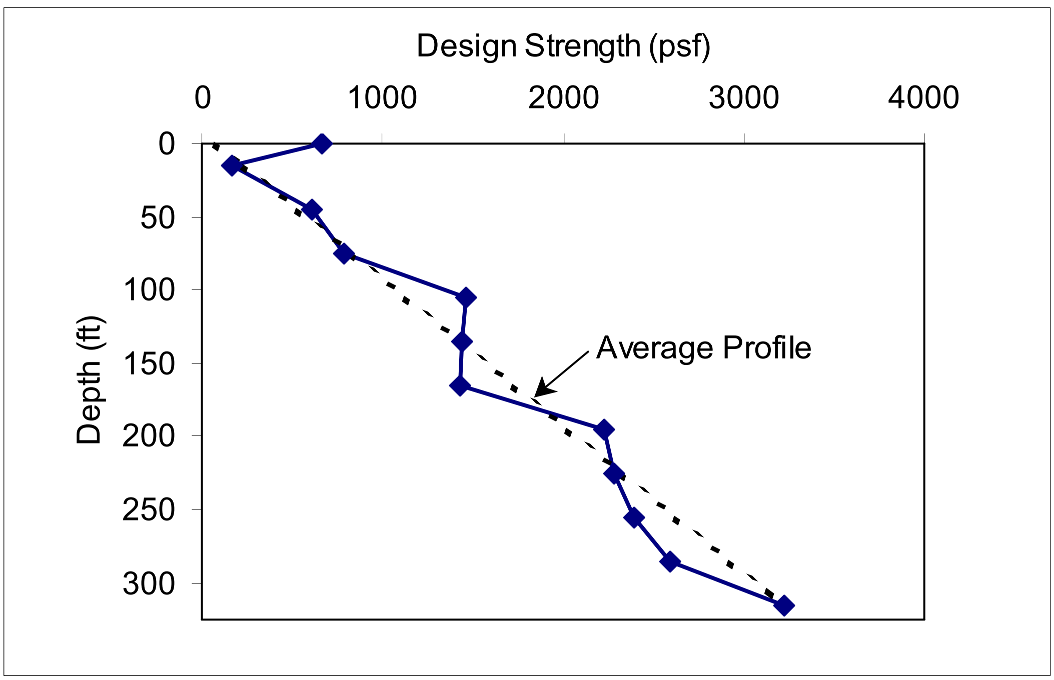

Figure 4. Example of simulated strength profile.

Table 3. Comparison of total side friction for 25 simulated soil profiles.

	Suction Caisson	Driven Pile
Average Total Side Friction (kips)	650	3,000
Standard Deviation in Total Side Friction (kips)	88	250
Coefficient of Variation in Total Side Friction	14 %	8 %

Table 4. Comparison of net end bearing for 25 simulated soil profile.s

	Suction Caisson	Driven Pile
Average Net End Bearing (kips)	580	250
Standard Deviation in Net End Bearing (kips)	230	58
Coefficient of Variation in Net End Bearing	39 %	23 %
Average Contribution to Total Capacity	42 %	7 %

Table 5. Variability in total capacity for 25 simulated soil profiles.

	Suction Caisson	Driven Pile
Coefficient of Variation in Axial Capacity	21 %	8 %
Coefficient of Variation in Lateral Capacity	33 %	Not Relevant

Calibration of Suction Caisson Design Method

In order to understand the effect of uncertainty from site characterization programs on design, the first step is to assess the magnitude of uncertainty in the design method itself (i.e., even if a soil boring exists at the location of a suction caisson, the actual capacity is still uncertain due to uncertainty in the design method). In this way, the relative contribution of uncertainty that can be controlled through site characterization is considered in the proper perspective of the overall uncertainty in the design capacity.

Design methods and criteria for the capacity of suction caissons have generally been adapted from those for driven pipe piles (Andersen et al. 1999). However, the accuracy of these design methods has never been thoroughly tested due to the lack of published databases of pullout tests on suction caissons. A database that is comprised of published laboratory model tests, centrifuge tests, and full scale field tests conducted on suction caissons in normally consolidated clays was assembled and used to evaluate biases and uncertainties that are inherent in available models for predicting the uplift capacity of suction caissons in normally consolidated clays.

Capacity for Axial (Uplift) Loading

The axial capacity of a suction caisson, which generally governs design in practical applications even for inclined loading conditions, is comprised of side shear and reverse end bearing. Under rapid uplift loading, the side resistance is typically calculated using a variation of the alpha method as a function of the undrained shearing strength of the soil. For normally consolidated clays, an alpha value of near 1.0 is typically used in the design of offshore piles. For suction caissons, concerns about the effect of suction installation, soil setup, and the presence of the padeye have led to a tendency for designers to reduce alpha to values that are less than 1.0 (α = 0.6 to 0.8). Randolph and House (2002) indicate that after installation, the external side resistance is expected to increase from the soil's remolded strength to a fully equalized strength that corresponds to alpha values of about 0.5 to 0.7. The fact that alpha does not reach a value of 1.0 is attributed by the authors to the high ratio of diameter to wall thickness of suction caissons. Andersen and Jostad (1999) and Clukey (2001) state that an expected reduction in the external skin friction for the full set-up condition can be attributed to a reduction in soil stresses on the portion of the caisson that is installed with suction. The rationale behind such a concern is the observation that the soil typically moves into the caisson (rather than outside the caisson) as a result of installation by suction.

The net reverse end bearing for rapid uplift loading is typically calculated by multiplying the undrained shearing strength at the tip of the caisson by an end bearing factor N, which for driven piles have been typically set to 9. For suction caissons, some studies indicate an end bearing factor that can be greater than 9 (Clukey and Morrison 1993, House and Randolph 2001, Randolph and House 2002 and Clukey et al. 2002, Luke et al. 2003). A major difference between driven piles and suction caissons lies in the relative contribution of the net reverse end bearing to the total capacity. For driven piles, the contribution of the net end bearing is typically less than 10%. For caissons with geometries that are typical of those used in the Gulf of Mexico, the net reverse end bearing can account for about 40% to 60% of the total axial capacity (Clukey and Phillips 2002).

In order to calibrate the design parameters □ and N, a database of load tests was compiled. General information about the type of soil, geometry of the caisson, and loading conditions is presented in Table 6, while specific information regarding properties of the soil and measured capacities is presented in Table 7. Details regarding each test are presented in Najjar (2005).

Table 6. Database of pullout tests on suction caissons (general description).

#	Caisson ID	Soil Type	Diam feet	L/D	Accel. g's	Top Cap	Loading	Rate of Loading mm/sec	Setup
1	Luke et al 2003	Kaolinite	0.33	8.2	1 g	Vented	Monotonic	5 to 20	48 hrs
2	Luke et al 2003	Kaolinite	0.33	8.1	1 g	Vented	Monotonic	5 to 20	48 hrs
3	Luke et al 2003	Kaolinite	0.33	8.0	1 g	Vented	Monotonic	5 to 20	48 hrs
4	Luke et al 2003	Kaolinite	0.33	8.4	1 g	Closed	Monotonic	5 to 20	48 hrs
5	Luke et al 2003	Kaolinite	0.33	8.1	1 g	Closed	Monotonic	5 to 20	48 hrs
6	Luke et al 2003	Kaolinite	0.33	8.0	1 g	Closed	Monotonic	5 to 20	48 hrs
7	Luke et al 2003	Kaolinite	0.33	7.8	1 g	Closed	Monotonic	5 to 20	48 hrs
8	Clukey 1993	Kaolinite	49.9*	2.1	100g	Closed	Monotonic	2.6 to 4.1 days*	24 hrs
9	Clukey 1993	Kaolinite	49.9*	2.1	100g	Closed	Monotonic	14 days*	24 hrs
10	Clukey 1993	Kaolinite	49.9*	2.1	100g	Closed	Monotonic	2.6 to 4.1 days*	24 hrs
11	House 2002	Kaolinite	11.81*	4.0	120g	Vented	Monotonic	0.1	0
12	House 2002	Kaolinite	11.81*	4.0	120g	Closed	Monotonic	0.3	0
13	House 2002	Kaolinite	11.81*	4.0	120g	Closed	Sustained	150 days*	0
14	Randolph 2001	Kaolinite	11.81*	3.9	120g	Vented	Sustained	0.1 (10 days*)	0
15	Randolph 2001	Kaolinite	11.81*	3.9	120g	Vented	Sustained	6 months*	1 year*
16	Randolph 2001	Kaolinite	11.81*	3.9	120g	Closed	Monotonic	0.3	7 days*
17	Randolph 2001	Kaolinite	11.81*	3.9	120g	Closed	Cyclic	-	1 year*
18	Randolph 2001	Kaolinite	11.81*	3.9	120g	Closed	Sustained	Long term*	1 year*
19	Clukey 2002	Kaolinite	17.4*	4.7	114g	Closed	Monotonic	8 sec	20 hrs
20	Clukey 2002	Kaolinite	17.4*	4.9	114g	Closed	Monotonic	8 sec	20 hrs
21	Clukey 2002	Kaolinite	17.4*	5.0	114g	Closed	Monotonic	8 sec	20 hrs
22	Clukey 2002	Kaolinite	17.4*	4.8	114g	Closed	Monotonic	8 sec	20 hrs
23	Cho et al 2003	CH-Clay	1.6	9.6	1 g	Closed	Monotonic	5 min	3 days
24	Cho et al 2003	CH-Clay	3.3	4.7	1 g	Closed	Monotonic	5 min	3 days
25	Cho et al 2003	CH-Clay	4.9	3.1	1 g	Closed	Monotonic	5 min	3 days

* Prototype Scale

Table 7. Database of pullout tests on suction caissons (soil properties and measured loads).

#	Caisson ID	Method of Shear Strength Measurement	Density pcf	Average S_u psf	Tip S_u psf	Sensitivity	Measured Capacity in Uplift kips
1	Luke et al. 2003	T-Bar	86.6	6.4	10.9	1.8	0.028
2	Luke et al. 2003	T-Bar	86.5	6.3	10.8	1.8	0.025
3	Luke et al. 2003	T-Bar	86.5	6.2	10.6	1.8	0.023
4	Luke et al. 2003	T-Bar	86.7	6.5	11.2	1.8	0.030
5	Luke et al. 2003	T-Bar	86.5	6.3	10.7	1.8	0.029
6	Luke et al. 2003	T-Bar	86.5	6.2	10.6	1.8	0.028
7	Luke et al. 2003	T-Bar	86.4	6.1	10.4	1.8	0.030
8	Clukey 1993	CPT to Vane*	108	565	1080	2.0	24615
9	Clukey 1993	CPT to Vane*	108	565	1080	2.0	23964
10	Clukey 1993	CPT to Vane*	108	565	1080	2.0	25905
11	House 2002	T-Bar	104.4	185	370	2.0	427
12	House 2002	T-Bar	104.4	200	400	2.0	748
13	House 2002	T-Bar	104.4	215	430	2.0	748
14	Randolph 2001	T-Bar	104.4	185	370	2.0	354
15	Randolph 2001	T-Bar	104.4	185	370	2.0	618
16	Randolph 2001	T-Bar	104.4	185	370	2.0	755
17	Randolph 2001	T-Bar	104.4	185	370	2.0	697
18	Randolph 2001	T-Bar	104.4	185	370	2.0	572
19	Clukey 2002	Piezo. to DSS**	108	328	625	2.0	3324
20	Clukey 2002	Piezo. to DSS**	108	360	690.00	2.0	3480
21	Clukey 2002	Piezo. to DSS**	108	363	693.00	2.0	3258
22	Clukey 2002	Piezo. to DSS**	108	344	658.00	2.0	3370
23	Cho et al 2003	UU -Triaxial	92	125.28	142	2.0***	12
24	Cho et al 2003	UU- Triaxial	92	125.28	142	2.0***	35
25	Cho et al 2003	UU- Triaxial	92	125.28	142	2.0***	82

CPT calibrated to Vane, ** Piezocone calibrated to Direct Simple Shear, *** Assumed value

The database is comprised of seven lab-scale model tests, fifteen centrifuge tests, and three full scale field tests. Diameters range from 4 inches (model tests) to about 50 feet (prototype scale for centrifuge tests), while aspect ratios range from 2 to 10. In all the lab and centrifuge tests, kaolinite is used to model the soil profile. The majority of load tests in the database are conducted under rapid monotonic loading conditions to simulate undrained uplift under environmental loading conditions in the field. However, different loading rates are used in different studies, thus introducing a source of uncertainty in the measured loads. Another source of uncertainty in the database is the different periods of time that were allowed for the suction caissons to setup prior to undrained testing. Load tests that are conducted prior to full equalization of excess pore water pressures that result from the installation process can underestimate the ultimate capacity of the caisson. A last major source of uncertainty in the database lies in the use of different methods to measure the undrained shearing strength of the soil. A variety of direct simple shear, unconsolidated-undrained triaxial, cone penetration, vane shear, and T-bar tests are used to measure the undrained shearing strength in the different case studies analyzed.

In an initial analysis of the database, predicted capacities for the 25 tests were calculated using □ = 1 and N = 9. Values of undrained strength that were reported in the original references were used in this initial analysis with no attempts to correct for the method of shear strength measurement. For pullout tests that were conducted immediately after installation (Tests 11 to 14), the undrained shearing strength of the remolded clay was used in calculating the predicted side shear capacity. Ratios of measured to predicted capacities for the 25 tests in the database are plotted on Figure 1. Results on Figure 5 indicate an average ratio of measured to predicted capacity of 0.99 (unbiased model) and a coefficient of variation in the ratio of measured to predicted capacity of 0.28.

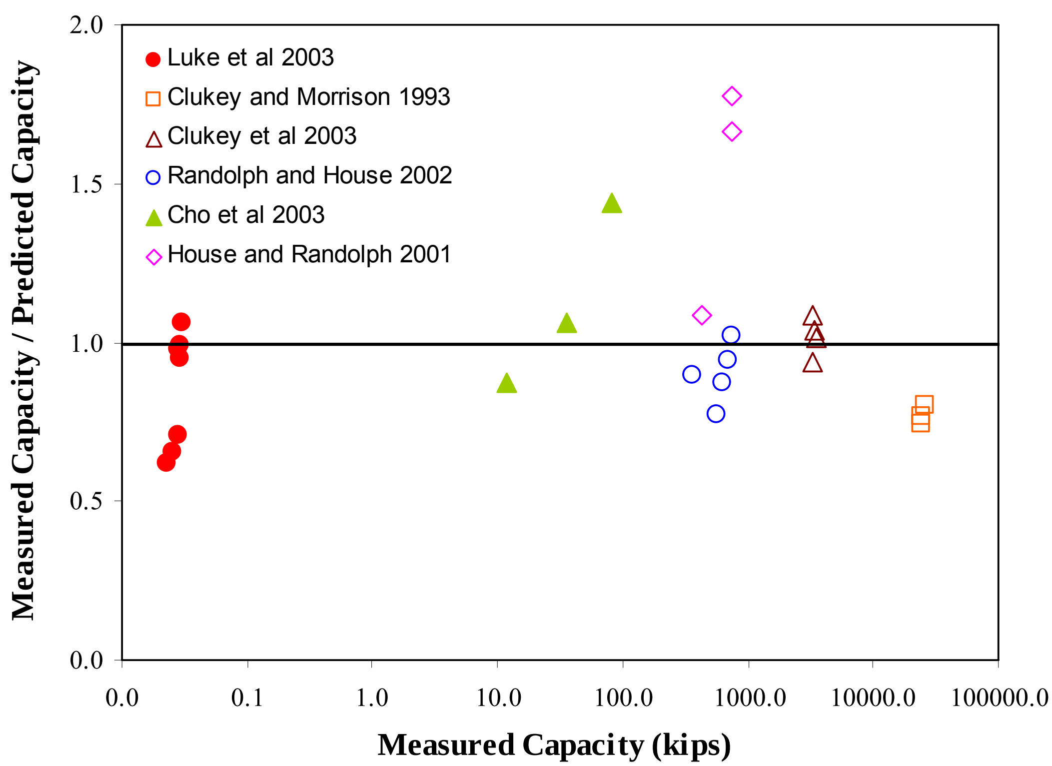

Figure 5. Comparison between measured and predicted capacities for 25 suction caissons (uncorrected shear strength, α = 1, N = 9).

In the majority of tests in the database, the undrained shear strength is measured using T-bar penetration tests (using T-bar factors of 10.5) and the values are expected to correlate well with shear strength values measured using the direct simple shear test (Watson et al. 2000). To provide a consistent analysis of the data, a correction factor F_c is introduced to calculate an equivalent standard undrained shear strength. Since most of the cases in the database utilize the T-bar test, and since results from T-bar tests are expected to correlate well to results from direct simple shear tests, the correction factor is defined as the ratio of the shear strength determined using direct simple shear tests to the shearing strength measured using some other technique. Generally, undrained shear strength values that are measured in direct simple shear tests are about 70% to 80% of shear strength values obtained from triaxial compression tests and vane shear tests (Watson et al. 2000). As a result, an F_c value of 0.75 was used to calculate equivalent undrained shear strengths for the tests reported by Clukey and Morrison (1993) and Cho et al. (2003). In addition, values of undrained strength for the tests reported by Clukey et al. (2003) are increased by 20%, based on the recommendations of the authors, to account for differences in the shearing rates used in the direct simple shear tests and the centrifuge pullout tests. The centrifuge tests were conducted at a rate that was 1000 times faster than the shearing rate used in the direct simple shear tests. Additional direct simple shear tests that were conducted at higher rates of loading indicated a 7% increase in the undrained shear strength per log cycle of loading.

The ratio of measured to predicted capacities was reevaluated for the 25 tests using a corrected undrained shear strength (the equivalent of that measured in a direct simple shear test) with □ = 1 and N = 9; the results are plotted on Figure 6. Results indicate a small difference due to the effect of using corrected undrained shear strengths, with an average ratio of measured to predicted capacity of 1.03 (compared to 0.98) and a coefficient of variation in the ratio of measured to predicted capacity of 0.31 (compared to 0.28).

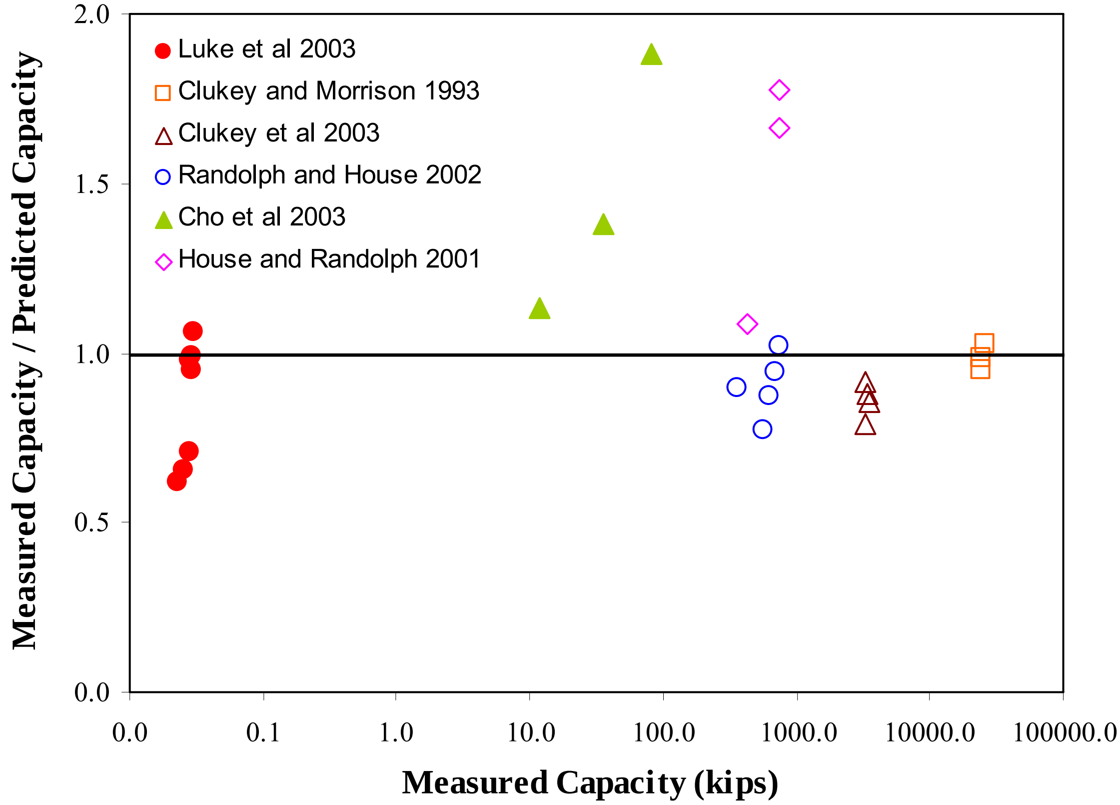

Figure 6. Comparison between measured and predicted capacities for 25 suction caissons (corrected undrained shear strength for direct simple shear, α = 1, N = 9).

This initial analysis indicated that an alpha of 1 and an end bearing factor of 9 can be used to calculate an approximately unbiased estimate of the capacity of suction caissons in normally consolidated clay. The uncertainty in the model can be represented with a coefficient of variation of 0.3 in the ratio of measured to predicted capacity.

A more detailed analysis of the data was conducted by (1) disregarding tests that were conducted immediately after installation, and (2) distinguishing between tests conducted on sealed and vented caissons. The calculated values of the mean and coefficient of variation of the ratio of measured to predicted capacity for each test case are summarized in Table 8. Results in Table 8 indicate that (1) for the four vented tests in which a seemingly adequate setup time was allowed prior to load testing, predictions of the uplift capacity using an alpha of 1 tend to overestimate the capacity by about 30%, (2) for the 17 sealed tests in which a seemingly adequate setup time was allowed prior to load testing, predictions using an alpha of 1 and an end bearing factor of 9 provide a relatively unbiased prediction of capacity, and (3) when only the 17 sealed tests are analyzed, the uncertainty in the prediction model decreases noticeably; the coefficient of variation in the ratio of the measured to predicted capacity decreases to 0.17 or 0.25, depending on whether the uncorrected or corrected undrained shear strength values are used in predicting capacity.

Table 8. Biases and uncertainties in model for suction caissons (α=1, N=9).

		Number of Tests	Average for Ratio of Measured to Predicted	Coefficient of Variation for Ratio of Measured to Predicted
Uncorrected Undrained Shear Strength	All Tests	25	0.99	0.28
	All Tests with Setup	21	0.92	0.20
	Sealed Tests with Setup	17	0.97	0.17
	Vented Tests with Setup	4	0.71	0.16
Corrected Direct Simple Shear Strength	All Tests	25	1.03	0.31
	All Tests with Setup	21	0.97	0.28
	Sealed Tests with Setup	17	1.03	0.25
	Vented Tests with Setup	4	0.71	0.16

While values of $\alpha = 1$ and $N = 9$ provide reasonably unbiased results, there is actually a range of combinations of $\alpha = 1$ and $N = 9$ that can produce unbiased results since a single value, the total axial capacity, is measured in the load tests. Combinations of α and N that resulted in an unbiased model were calculated and presented in Table 9. Coefficients of variation in the ratio of measured to predicted capacity corresponding to these combinations of α and N were also calculated (Table 9). Tests where the caissons were pulled out immediately after installation (no set up) were excluded from the analysis. Results indicate that different combinations of α and N can be used to predict the measured capacities in an unbiased manner. For values of α ranging from 0.7 to 1, the corresponding N factors range from 13 to 8.5, respectively, while corresponding c.o.v's range from 0.26 to 0.28. It should be noted that the combination of α = 0.7 and N = 13 provides an unbiased estimate for both the vented tests and the sealed tests even when analyzed separately.

Table 9. Calibration of α and N (corrected undrained shear strength and excluding tests with setup = 0).

		Measured Capacity / Predicted Capacity	
α	**N**	**Average**	**Coefficient of Variation**
1.0	8.5	1.0	0.28
0.9	9.7	1.0	0.27
0.8	11.2	1.0	0.26
0.7	13	1.0	0.26

As a final piece of information on the calibrated design method, El-Sherbiny (2005) conducted 1-g model tests with a double-walled caisson where the contribution of side shear and end bearing could be separated. El-Sherbiny found from four tests that an average alpha of 0.78 and an average N of 15 were mobilized at the failure load. Conversely, Jeanjean et al. (2006) conducted centrifuge model tests with a double-walled caisson and measured an alpha of 0.85 and N of 9. Jeanjean et al. (2006) actually measured a value greater than 12 for N at a displacement of about 10% of the caisson diameter; however, the maximum side shear was mobilized at about one-tenth of that displacement. Chen and Randolph (2005) reported an alpha factor of 0.76 and an N value of 12 to match their test results.

Therefore, the appropriate combination of alpha and N is on the order of □ = 0.8 and N = 12 based on all of the available information. This combination will produce a reasonably unbiased estimate of the uplift capacity for a suction caisson, with a coefficient of variation of about 0.3 between the actual and estimated capacity. For comparison purposes, similar analyses for driven piles produce a coefficient of variation for the design method that is between 0.2 and 0.3 (Najjar 2005).

Capacity for Lateral and Inclined Loading

The capacity for suction caissons on lateral and inclined loading is calculated using a combination of the method described and calibrated above for axial capacity and a method developed by Aubeny and Murff on an OTRC project at TAMU (referred to here s the SAIL method). In order to provide information for calibrating the SAIL method, El-Sherbiny (2005) ran a series of seven 1-g model tests with undrained loading and a loa attachment at the lower third point of the caisson (typical for practice). The tests covered the entire range of angles from horizontal to vertical, which provides a complete set of data for verification of the design method. The experimental results, shown on Fig. 7, compare very well with analyses performed using the SAIL method with = 0.78 and N = 15.

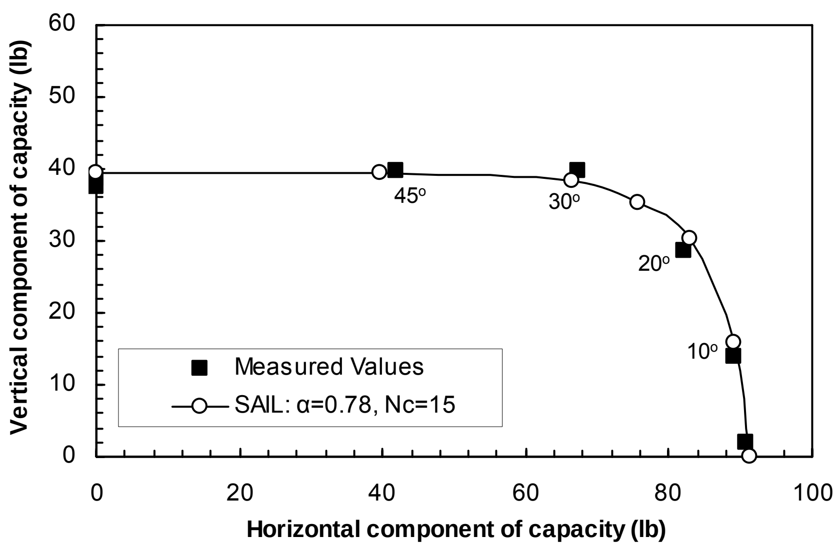

Figure 7. Comparison between measured and predicted components of suction caisson capacity under inclined loading (El-Sherbiny 2005).

Lower-Bound Capacity

One general concern arising from the work on spatial variability and model calibration is the magnitude of uncertainty for suction caisson design is generally larger than that for driven piles in normally consolidated clays. One possible mitigating factor is the effect of a lower-bound capacity in limiting the uncertainty (e.g., Gilbert 2003, Najjar 2005 and Gilbert et al. 2005).

The first step in investigating the effect of a lower-bound capacity was to re-evaluate load-test databases with driven piles, since the design methods for suction caissons were derived from those for driven piles. These databases show clear evidence for the existence of a lower-bound capacity in both cohesive and cohesionless soils (Gilbert et al. 2005 and Najjar 2005). This lower-bound capacity is a physical variable that can be calculated based on mechanics with site-specific soil properties. The calculated lower-bound capacity typically ranges from 0.5 to 0.9 times the calculated predicted capacity.

In order to explore the hypothesis of a lower-bound capacity for suction caissons in normally consolidated clay, an analysis is presented for the axial pullout tests available in the database (Tables 1 and 2). The predicted lower-bound capacity is calculated using the alpha method by replacing the undisturbed undrained shear strength with the remolded undrained shear strength of the soil. The remolded strength is calculated by dividing the undisturbed strength by the sensitivity of the soil. An alpha value of 1.0 and an end bearing factor of 9.0 is used in the analysis. In tests in which the top cap of the caisson is vented, 1-g model tests and centrifuge tests indicate a failure mode in which the caisson is pulled out without the formation of a plug. For these cases, the lower-bound side friction is calculated as the sum of frictional resistance acting on the inner and outer walls of the caisson and the lower-bound reverse end bearing is assumed to act on the annulus of the caisson. In tests in which the top cap is sealed, tests indicated the formation of a plug. For these cases, the lower-bound side friction is calculated from the external skin friction and the lower-bound reverse end bearing is assumed to act on the full cross sectional area of the caisson.

The ratio of the predicted lower-bound capacity to the measured capacity is calculated and plotted on Figure 8 for the 25 load tests shown on Figures 5 and 6. For all the cases studied, the calculated ratio of the predicted lower-bound capacity to the measured capacity is less than 1.0, indicating clear evidence for the existence of a lower-bound axial capacity. The ratio of lower-bound capacities to measured capacities ranged from 0.25 to 1.0 and had an average value of 0.62. The incorporation of lower-bound capacities of this magnitude into reliability analyses can have a significant effect on the calculated reliability of suction caissons in normally consolidated clays. This effect is considered in the next section of this report.

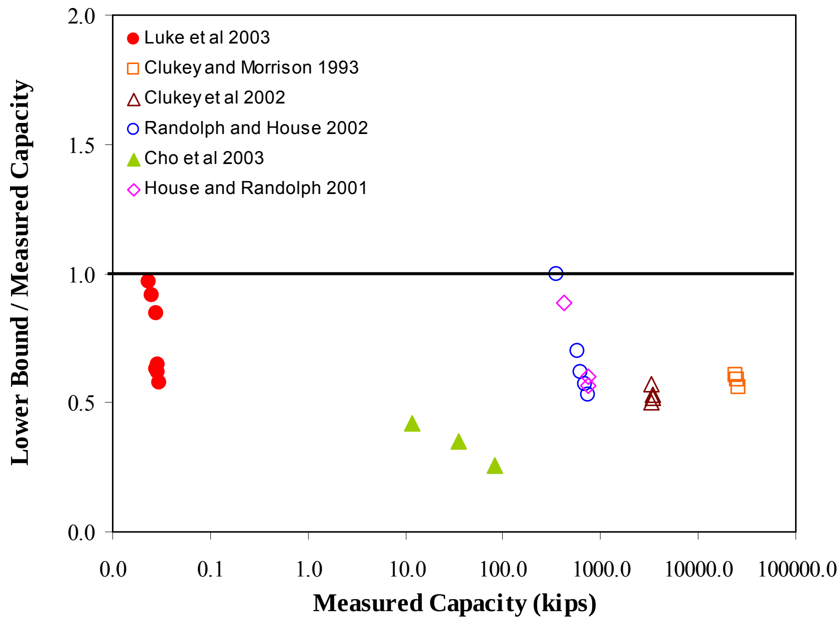

Figure 8. Evidence of Lower-Bound Capacity for 25 Suction Caissons

Reliability-Based Design of Suction Caissons

A conventional reliability analysis for an offshore foundation provides a useful framework as a starting point to consider the reliability of the suction caissons for the study spar. A conventional reliability analysis can be generalized in a convenient mathematical form as follows:

$$P\left(\text{Load>Capacity}\right) \cong \Phi\left(-\frac{\ln\left(FS_{\text{median}}\right)}{\sqrt{\delta_{\text{load}}^{2}+\delta_{\text{capacity}}^{2}}}\right) \tag{1}$$

where P(Load > Capacity) is the probability that the load exceeds the capacity in the design life, which is also referred to as the lifetime probability of failure; FS_{median} is the median factor of safety, which is defined as the ratio of the median capacity to the median load; and δ is the coefficient of variation (c.o.v.), which is defined as the standard deviation divided by the mean value for that variable. Equation 1 assumes that the load and capacity each follow lognormal distributions, a common assumption in typical reliability analyses for offshore foundations (e.g., Tang and Gilbert 1993).

The median factor of safety in Equation 1 can be related to the factor of safety used in design:

$$FS_{\text{median}} = FS_{\text{design}} \times \frac{\left(\dfrac{\text{capacity}_{\text{median}}}{\text{capacity}_{\text{design}}}\right)}{\left(\dfrac{\text{load}_{\text{median}}}{\text{load}_{\text{design}}}\right)} \tag{2}$$

where the subscript "design" indicates the value used to design the foundation. The ratios of the median to design values represent biases between the median or most likely value in the design life and the value that is used in the design check with the factor of safety. For context, the median factor of safety is between three and five for a pile in a typical jacket platform.

The coefficients of variation in Equation 1 represent uncertainty in the load and the capacity. For an offshore foundation, the uncertainty in the load is generally due to variations in the occurrence and strength of hurricanes at the platform site over the design life. The uncertainty in the capacity is due primarily to variations between the actual capacity in a storm load compared to the capacity predicted using the design method. The denominator in Equation 1 is referred to as the total coefficient of variation:

$$\delta_{total} = \sqrt{\delta^2_{load} + \delta^2_{capacity}} \tag{3}$$

As an example, typical c.o.v. values for a jacket platform range from 0.3 to 0.5 for the load, 0.3 to 0.5 for the capacity, and 0.5 to 0.7 for the total.

The relationship between the probability of failure and the median factor of safety and the total c.o.v. is shown on Figure 9. An increase in the median factor of safety and a decrease in the total c.o.v. both reduce the probability of failure. For context, the lifetime failure probabilities for a pile in a typical jacket foundation range from 0.005 to 0.05 (Fig. 9). Note that the event of foundation failure, i.e. axial overload of a single pile in the foundation, does not necessarily lead to collapse of a jacket. Failure probabilities for the foundation system are ten to 100 times smaller than those for a single pile (Tang and Gilbert 1993).

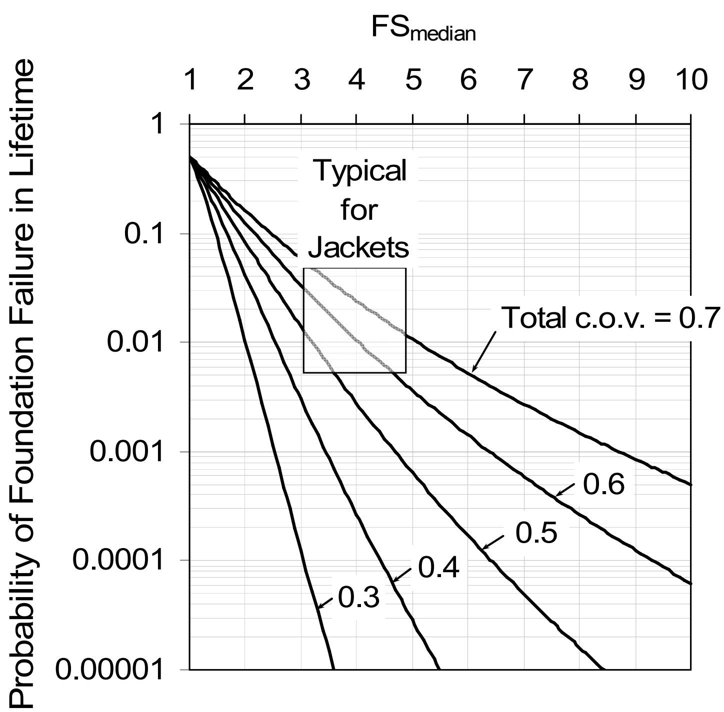

Figure 9. Results from a conventional reliability analysis on a pile in a typical jacket platform.

Bias and C.o.v. Values for Deepwater Mooring Systems

The reliability for a typical foundation in a deepwater mooring system will depend on appropriate values for the bias and c.o.v. values for the load and capacity (Fig. 9).

Foundation Load

In order to investigate loads, the results from a separate OTRC study on mooring system reliability were used (Zhang and Gilbert 2006). A numerical model (Ding et al. 2003) was used to simulate mooring line loads during different sea states for a study spar. From the resulting time histories and a probabilistic description of hurricanes for the Gulf of Mexico (Winterstein and Kumar 1995), a probability distribution was developed for the maximum load in a line during a storm (Dangayach 2004). The vertical load at the anchor was then determined from the maximum load and corresponding angle in the mooring line at the mudline using the analytical model developed by Neubecker and Randolph (1995). The results are summarized in Table 10 for the most heavily loaded line during a storm.

The conservative bias in the median load versus the design load is greater for these spar foundations than for a pile in a typical jacket platform, where the ratio of the median to the design load is between 0.7 and 0.8 (Tang and Gilbert 1993). This conservative bias is especially significant for the semi-taut mooring system (1,000-m water depth) due to the effect of removing a line in establishing the design load. The loads are shared more evenly between the lines in the taut mooring systems, which minimizes the impact on each line when one line is removed.

Table 10. Bias and c.o.v. values for foundation in study spar.

	Water Depth (m)		
	1,000	2,000	3,000
$load_{median}/load_{design(damage)}$	0.41	0.70	0.71
$capacity_{median}/capacity_{design}$	1.2 – 1.4	1.2 – 1.4	1.2 – 1.4
$FS_{design(damage)}$	1.5 - 2.5	1.5 - 2.5	1.5 - 2.5
FS_{median}	4 – 8	3 – 5	3 – 5
$\square_{load}$	0.30	0.14	0.11
$\square_{capacity}$	0.3	0.3	0.3
$\square_{total}$	0.4	0.3	0.3

Notes: Design life = 20 years; Axial loading governs design capacity.

Also, the coefficients of variation in the spar foundation load are smaller than for a pile in a typical jacket platform, where the c.o.v. values are generally between 0.3 and 0.5 (Tang and Gilbert 1993). There are several reasons for smaller uncertainty in the foundation loads on the spar. First, the line loads are less sensitive to wave height for a spar mooring system in deep water compared to a fixed jacket in shallow water (e.g., Banon and Harding 1989). Therefore, variations in the sea states over the design life are less significant for the spar mooring system. Second, the mooring system is simpler to model than a jacket, meaning that there is less uncertainty in the loads predicted by the model. Finally, the spar line loads are dominated by pre-tension versus environmental loads; variations in the load due to variations in the sea states therefore have a smaller effect on the total line load. This effect of pre-tension is particularly significant for the taut mooring systems (2,000-m and 3,000-m water depths), which consequently have the smallest c.o.v. values (Table 1).

Foundation Capacity

The work described above on spatial variability and calibrating the design method provide a basis for establishing the coefficient of variation in the capacity. For c.o.v. values of 0.25 to 0.3 in the design method and 0.1 to 0.2 for spatial variability due to soil borings not located at each foundation site, the total c.o.v. in capacity is 0.3 to 0.35. This value is very similar to the value of 0.3 that is typically used for pile foundations on jacket platforms (Tang and Gilbert 1993).

Median Factor of Safety, Total c.o.v. and Reliability

The biases in the load and the capacity are combined together with the design factor of safety through Equation 2 to determine the median factor of safety, and the results are summarized in Table 10. Typical factors of safety being used in practice for the damage case, which governs design for the study spar, range between 1.5 and 2.5. In addition, the total c.o.v. values are obtained from Equation 3 (Table 10).

The relationship between the reliability and FS_{median} and δ_{total} is re-plotted on Figure 10. For the spar foundation, the probability that the axial load will exceed the capacity of the suction caisson during a 20-year design life is on the order of 0.0001 or smaller. For comparison, this failure probability is more than two orders of magnitude smaller than that for piles in typical jacket structures (Fig. 10).

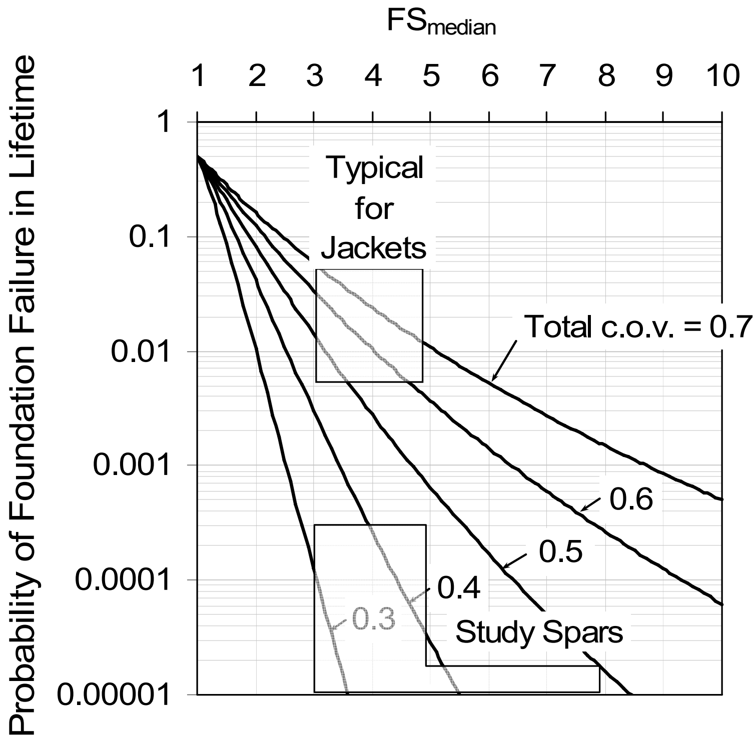

Figure 10. Results from a conventional reliability analysis on study spar foundations.

There are several reasons for the difference in reliability on Figure 10 between suction caisson anchors for floating production systems and piles in jacket platforms. A new source of conservatism was introduced for floating production systems with the damage case, where the factor of safety is applied to a load corresponding to one line missing. In addition, due to concerns with using new types of foundations such as suction caissons, the factors of safety were generally increased. Finally, there tends to be less uncertainty in the loads on mooring system anchors compared with jacket piles. The result of increased conservatism and decreased uncertainty for anchors compared to jacket piles is reflected on Figure 10.

Lower-Bound Foundation Capacity

A convenient and realistic mathematical model for the probability distribution of suction caisson capacity is shown on Figure 11 (Najjar et al. 2005). For capacities greater than the lower bound, the distribution is a continuous probability density function that follows a lognormal distribution. Most reliability analyses for pile capacities have assumed lognormal distributions for the pile capacity based on the available database information, and the model on Fig. 11 is consistent with this conventional approach. For capacities at the lower bound, there is a finite probability (that is, a probability mass function) that corresponds to the probability of being less than or equal to the lower bound in the non-truncated lognormal distribution.

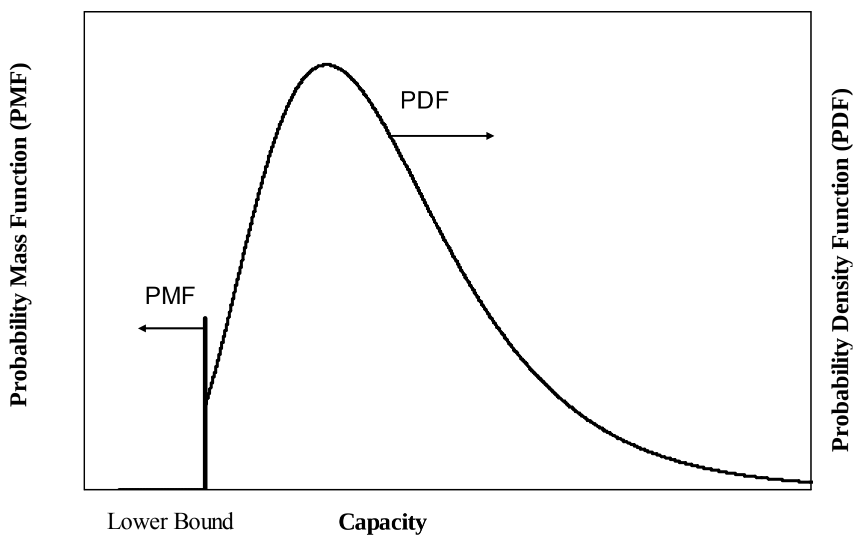

Figure 11. Mixed probability distribution for modeling suction caisson capacity.

Curves showing the variation of the reliability of a suction caisson foundation as a function of the ratio of the lower-bound to median capacity are shown on Figure 12. The reliability index (β) is defined as $\beta = -\Phi^{-1}(p_f)$, where p_f is the probability that the load exceeds the capacity and $\Phi^{-1}()$ is the inverse of the cumulative standard normal function. The curves on Figure 12 represent the case were the uncertainty in the capacity (c.o.v. = 0.3) is relatively large compared to the uncertainty in the load (c.o.v. = 0.15), which is typical for deepwater mooring systems. The primary conclusion from Figure 12 is that a lower-bound capacity can have a significant effect on the calculated reliability.

To better illustrate the magnitude of the effect of the lower-bound capacity, the median factor of safety that is required to achieve different levels of reliability are plotted on Figure 7 as a function of the ratio of the lower-bound to the median capacity. To highlight the importance of the lower-bound capacity, consider a typical lower-bound capacity of 0.6 times the median strength and a target reliability index of 4. The required median factor of safety from a conventional reliability analysis (that is, one that doesn't incorporate the lower-bound capacity) is 3.7. However, if the lower-bound capacity is incorporated into the analysis, the required median factor of safety is reduced to 2.7 while still maintaining the same level of reliability ($\beta = 4$). Results on Fig. 13 indicate that resistance factors in a Load and Resistance Factor Design (LRFD), which control the median factor of safety, may need to incorporate information about the lower-bound capacity if they are to provide a consistent level of reliability.

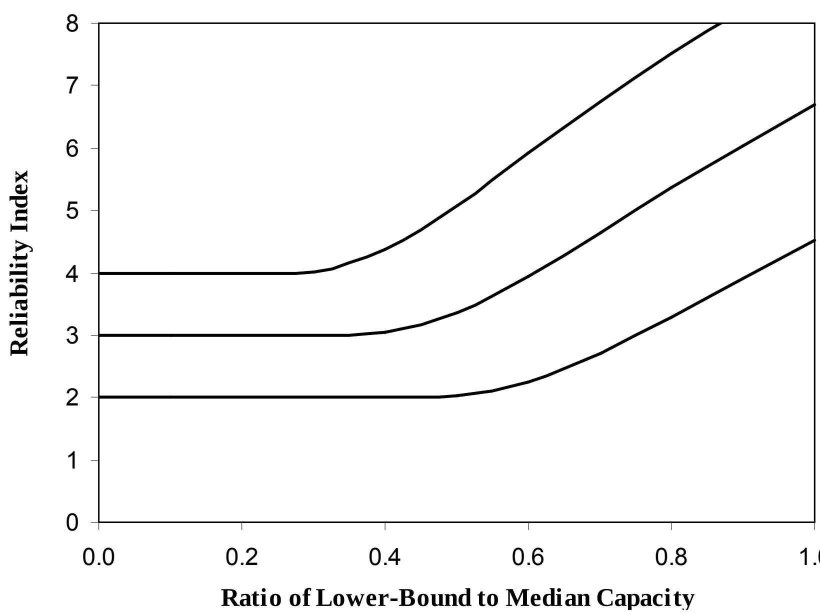

Figure 12. Effect of lower-bound capacity on reliability index ($c.o.v._{Load} = 0.15$, $c.o.v._{Capacity} = 0.3$).

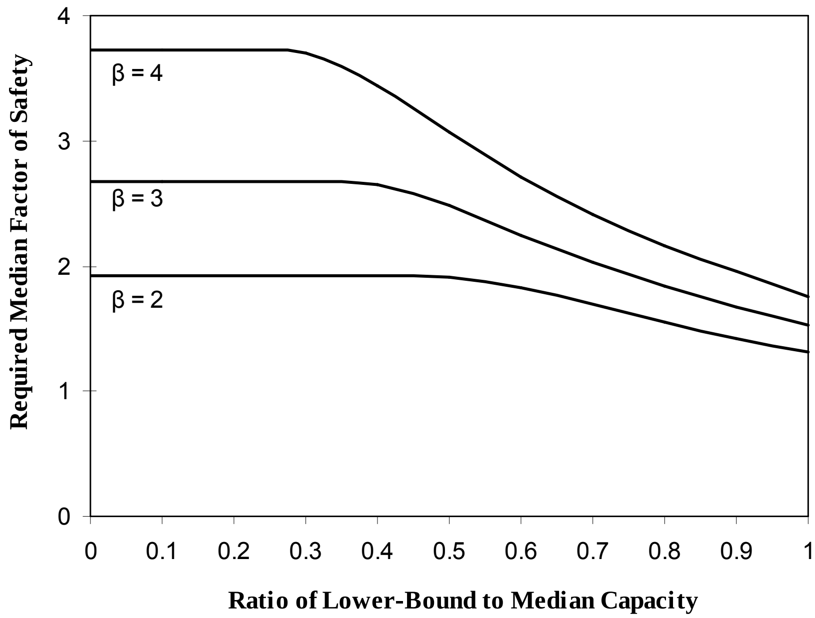

Figure 13. Variation of the required median factor of safety with the lower-bound capacity (c.o.v.$_{Load}$ = 0.15, c.o.v.$_{Capacity}$ = 0.3).

The effect of a lower-bound capacity on the reliability of the foundation is shown on Figure 14 for the study spar in 2,000 m of water. The results on Figure 14 show the significant role that a lower-bound capacity can have on the reliability. For the average lower-bound capacity from Figure 14, 0.6 times the median capacity, the probability of failure is more than 1,000 times smaller with the lower-bound than without it for a design factor of safety of 1.5 in the damage case. Furthermore, for design factors of safety of 2 or 2.5 in the damage case, the probability of failure for a lower-bound capacity that is 0.6 times the median capacity is essentially zero.

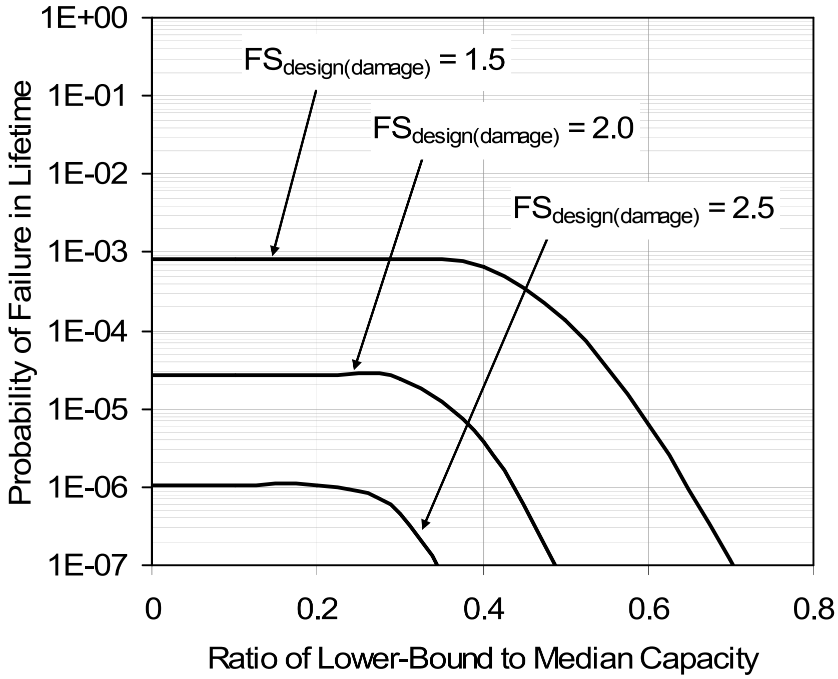

Figure 14. Effect of lower-bound capacity on probability of failure (study spar in 2,000-m water depth).

Target Reliability

Results from reliability analyses are generally presented in terms of the annual probability of an event in offshore applications. For example, Goodwin et al. (2000) recommend a target probability of failure of $2x10^{-4}$ per year for a single mooring line. The motivation for using annual probabilities is that many events in offshore applications, such as hurricanes and explosions, occur randomly with time. These annual probabilities of failure represent the rate of occurrence for high-consequence events.

In contrast to an event that is dominated by a time varying load, the uncertainty in the failure of an offshore foundation is dominated by uncertainty in the capacity. This capacity does not vary randomly with time. Therefore, it is not appropriate to consider the probability of failure as a rate of failure. If the actual capacity is higher than expected, then the annual rate of failure due to storm loading may be very small. If the actual capacity is lower than expected, then the annual rate of failure may be larger.

A more appropriate measure of the reliability for a foundation is the probability of failure during the lifetime of the structure. This probability was calculated in Figures 9, 10 and 14 by considering the time-varying component of the load to determine the distribution of the maximum load applied to the foundation over its lifetime.

In order to compare failure probabilities in a design life with target probabilities of failure that are expressed as annual rates, the target probabilities should be converted to a probability of failure in a lifetime. Since it is implicit in published failure rates that event occurrences are statistically independent with time, the probability of failure in a lifetime, T, can be obtained from the following:

$$\begin{aligned} P(\text{Load} > \text{Capacity in T years}) &= 1-(1-p_{\text{annual}})^T \\ &\cong Tp_{\text{annual}} \end{aligned} \quad (4)$$

where p_{annual} is the annual failure rate. Therefore, the target failure rate of 2×10^{-4} per year for a single mooring line recommended by Goodwin et al. (2000) corresponds to a target probability of failure of 0.004 in a 20-year design life.

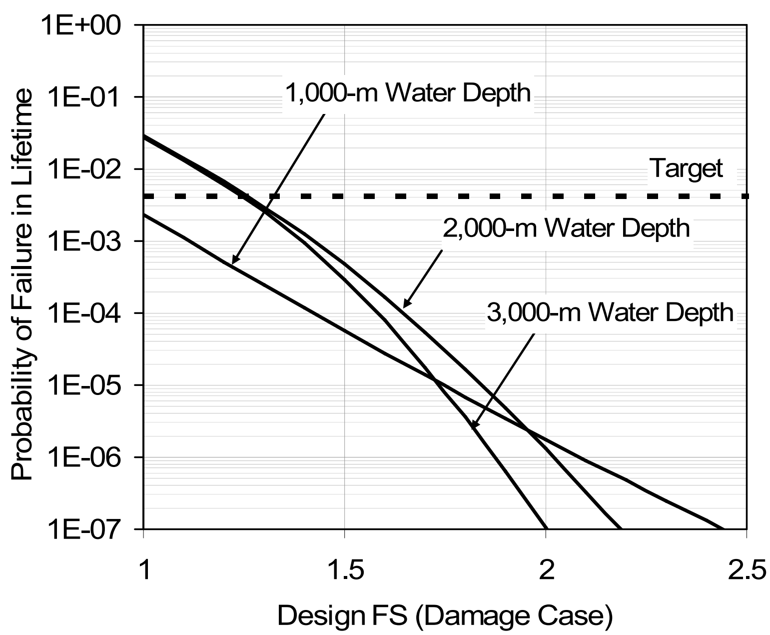

Figure 15. Reliability for study spar foundations versus design factor of safety (20-year design life).

The probability of failure in a lifetime is shown on Figure 15 for the study spar foundation in the three water depths. For these foundations, the lower-bound capacity was calculated to be about 0.43 times the median capacity. The target probability of failure is also shown on Figure 15. A factor of safety of 1.3 for the damage case would achieve the target reliability for all three water depths. In comparison, current practice has this factor of safety between 1.5 and 2.5.

Reliability-Based Design Considerations

Since a lower-bound capacity can have a significant effect on the reliability of a design, a reliability-based (or Load and Resistance Factor Design or LRFD) design code should include information on the lower-bound capacity. Two alternative formats are proposed here for including information about a lower-bound capacity in a LRFD design code: (1) a conventional design checking equation where the resistance factor (or design factor of safety) is adjusted according to the lower-bound capacity and (2) a second design checking equation to include information about the lower-bound capacity.

Adjusted Resistance Factor for Lower-Bound Capacity

The conventional LRFD design checking equation has the following general form:

$$\phi_R r_{nominal} \geq \gamma_Q q_{nominal} \tag{5}$$

where $r_{nominal}$ is the nominal capacity calculated using a design method, ϕ_R is the resistance factor, $q_{nominal}$ is the nominal load for design, and γ_Q is the load factor. In order to incorporate the effect of a lower-bound capacity, this design checking equation is modified as follows:

$$\phi_{R(r_{LB})} r_{nominal} \geq \gamma_Q q_{nominal} \tag{6}$$

where the resistance factor, $\phi_{R(r_{LB})}$, is a function of the lower-bound capacity. The ratio of the resistance factor incorporating a lower-bound capacity with the conventional resistance factor, $\phi_{R(r_{LB})}/\phi_R$, is shown as a function of the lower-bound capacity on Figure 16 for different target values of the reliability index. For reasonable values of the ratio of the lower-bound to median capacity, 0.4 to 0.9, the effect of the lower bound on the required resistance factor is significant.

In terms of a design based on factors of safety, the typical practice in the Gulf of Mexico, the effect of the lower bound on the factor of safety can be obtained by dividing the conventional factor of safety by the ratio of $\phi_{R(r_{LB})}/\phi_R$ on Figure 16. For example, if $\phi_{R(r_{LB})}/\phi_R$ is 1.2 from Fig. 16 based on the particulars of a specific design, then the factor of safety for the design could be reduced by 1/1.2 by accounting for the lower-bound capacity.

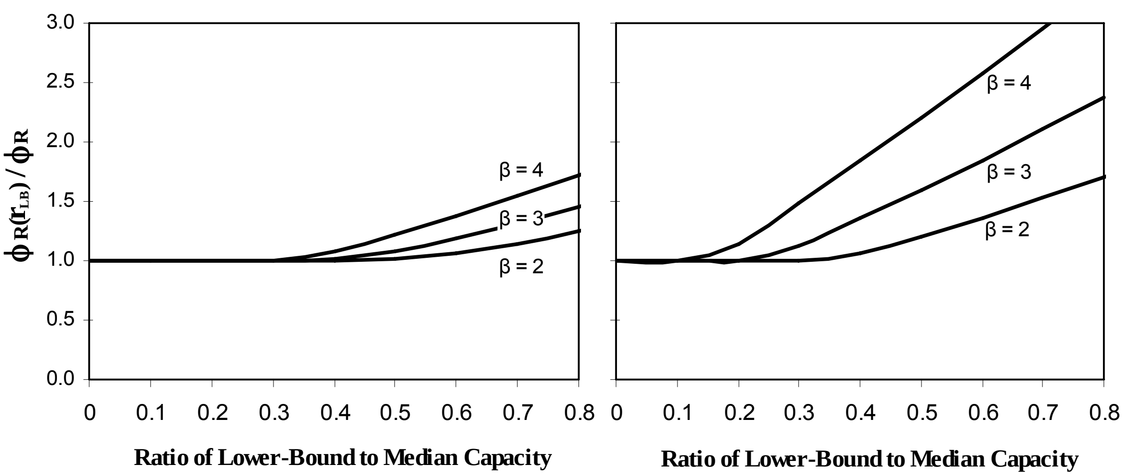

(a) c.o.v.$_{Capacity}$ = δ_R = 0.3 (b) c.o.v.$_{Capacity}$ = δ_R = 0.5

Figure 16. Variation of the increase in the nominal resistance factor with the lower-bound capacity (c.o.v.$_{Load}$ = δ_Q = 0.15).

Added Design Checking Equation for Lower-Bound Capacity

An alternative code format would be to have two design checking equations:

$$\begin{gathered}\phi_R r_{nominal} \geq \gamma_Q q_{nominal} \\ \text{OR} \\ \phi_{R_{LB}} r_{LB} \geq \gamma_Q q_{nominal}\end{gathered} \tag{7}$$

where the first design checking equation is the conventional equation and the second equation includes a resistance factor, $\phi_{R_{LB}}$, that is applied directly to the lower-bound capacity. Providing that one or the other of the two equations is satisfied, a design will provide the specified level of reliability. The motivation for this form of the design checking equation is that the conventional approach is incorporated and does not need to be modified, whether or not there is a lower-bound capacity; the effect of a lower-bound capacity is reflected entirely in the second equation.

A plot of $\phi_{R_{LB}}$ versus the lower-bound capacity is shown on Figure 17 for different target reliability indices. The curves begin at values of the lower-bound capacity, specifically r_{LB}/r_{median}, where the second design checking equation in Equation (7) governs. One advantage of this approach with two design checking equations (Equation 7 versus Equation 6) is that $\phi_{R_{LB}}$ is not very sensitive to either the magnitude of the lower-bound capacity or the target reliability index (Fig. 17). In fact, a conservative value of around 0.75 for $\phi_{R_{LB}}$ could be used to cover a wide range of possibilities.

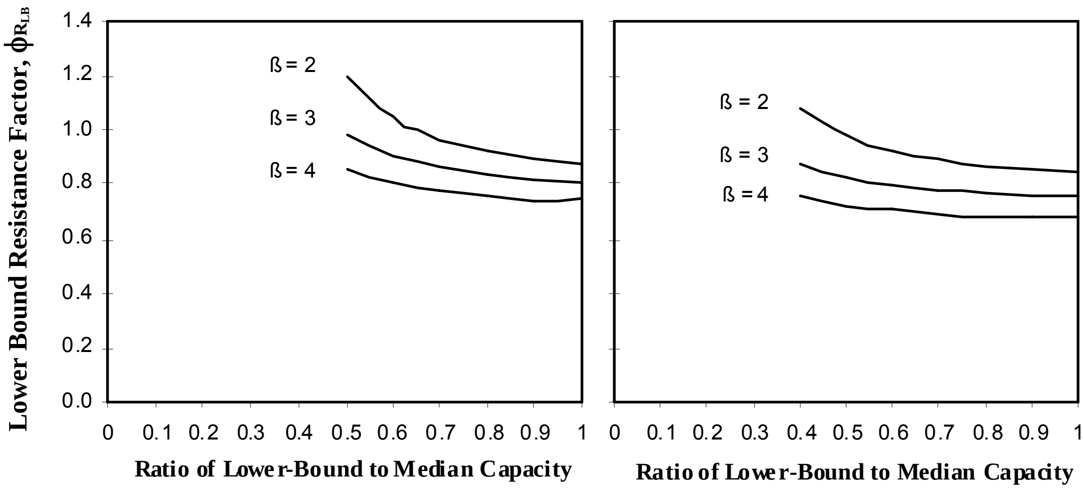

(a) c.o.v.$_{Capacity}$ = □$_R$ = 0.3 (b) c.o.v.$_{Capacity}$ = □$_R$ = 0.5

Figure 17. Variation of the lower-bound resistance factor to account for a lower-bound capacity (c.o.v.$_{Load}$ = $_Q$ = 0.15).

Value of Site Characterization and Installation Data

By considering all of the factors together in the design of a suction caisson, the relative importance of site characterization information can be assessed. In terms of capacity, the consequence of not having site-specific borings at every caisson location is relatively small. At most, the total c.o.v. in capacity would be reduced by about 80 percent (if the c.o.v. in the design method is 0.25 and the c.o.v. due to spatial variability is 0.2). However, when the load uncertainty, the effect of a lower-bound value on the caisson capacity, and the factors of safety are included, this reduction in uncertainty would be negligible for conventional design practice. Another way to say this is that the reliability that is being achieved in design practice is so high (Figs. 10 and 15) that there is plenty of room for relatively small variations in soil properties without impacting the reliability. However, site characterization data can play a much more significant role in foundation installation, which has not been addressed in this research.

On the other hand, the presence of a lower-bound value on the capacity can have a significant effect on the reliability (Fig. 14). Data on the lower-bound capacity can be obtained from caisson installation. Therefore, there is a significant potential to make designs more efficient and effective by making use of installation data to verify and update estimates of capacity. While outside the scope of this research, this approach would be particularly useful for Mobile Offshore Drilling Units.

Summary

Major conclusions from this work as follows:

1. The magnitude of spatial variability in the capacity of suction caissons depends substantially on the geologic setting. In normally consolidated marine clays in deepwater in the Gulf of Mexico, the absolute variability is small with coefficients of variation between 0.1 and 0.2. While small in an absolute sense, the magnitude of spatial variability in the capacity of suction caissons is greater than that for driven piles due to the effects of spatial averaging over the long length of a driven pile.

2. The uncertainty in design models for suction caissons is comparable to but slightly higher than that for driven piles in normally consolidated clays.

3. There is a physical lower-bound to the range of possible capacities, and this lower-bound can have a significant affect on the reliability of the foundation. One practical implication of this effect is to include a design check using the lower-bound capacity in addition to the nominal or design capacity. A second practical implication is that installation data can be used to update the reliability even when significant set-up is expected

4. Foundation designs for permanent floating production systems may be excessively conservative. The probability of failure values being achieved are several orders of magnitude smaller than industry-recommended targets for components (single line or foundation) in a mooring system. The practical concern with such excessive conservatism is that installation can become unnecessarily costly and problematic. In fact, if one suction caisson in the mooring spread cannot be installed, then the risk actually increases because the system is in a damaged state from the start.

5. The practice of not having geotechnical borings or probes at the location of every suction caisson in a facility layout does not adversely impact the reliability of the foundation because the effects of this uncertainty are negligible in light of the uncertainties in the loads, the presence of a lower-bound on the capacity, and the design factors of safety that are used today in practice.

References

Aubeny, C. P., Han, S., and Murff, J. D. (2003). Refined model for inclined load capacity of suction caissons. *Proceedings of the International Conference on Offshore Mechanics and Arctic Engineering*, OMAE, pages-5.

American Petroleum Institute: *Recommended Practice for Planning Designing, and constructing Fixed Platforms-Load and Resistance Factor Design*, RP 2A-LRDF, Washington D.C., 1993.

Banon, H. and Hardin, S. J. 1989. Methodology for Assessing Reliability of Tension Leg Platform Tethers. *Journal of Structural Engineering*, Vol. 115, No. 9: 2243 – 2259.

Bea, R. G., Jin, Z., Valle, C. and Ramos, R. 1999. Evaluation of Reliability of Platform Pile Foundations. *J. Geotech. and Geoenvir. Engrg.,* ASCE, 125(8): 696-704.

Chen, W. and Randolph, M. F. (2005), "Centrifuge Tests on Axial Capacity of Suction Caissons in Clay," *Proceedings of International Symposium on Frontiers in Offshore Geotechnics: ISFOG 2005, Perth, Australia.*

Cho, Y., Lee, T. H., Chung, E. S., and Bang, S. (2003). Field tests on pullout loading capacity of suction piles in clay. *Proceedings of the International Conference on Offshore Mechanics and Arctic Engineering*, OMAE, pages-7.

Clukey, E. C. (2001). Suction caisson design issues. *Proceedings of the OTRC International Conference*, 163-181.

Clukey, E. C., Aubeny, C. P., and Murff, J. D. (2003). Comparison of analytical and centrifuge model tests for suction caissons subjected to combined loads. *Proceedings of the International Conference on Offshore Mechanics and Arctic Engineering*, OMAE, pages-6.

Clukey, E. C., Banon, H. and Kulhawy, F. H. 2000. Reliability Assessment of Deepwater Suction Caissons. *Proc. Offshore Technology Conf., Houston, OTC 12192:* 777-785.

Clukey, E. C. and Morrison, M. J. (1993). A centrifuge and analytical study to evaluate suction caissons for TLP applications in the Gulf of Mexico. *Geotechnical Special Publication No. 38,* ASCE, 141-156.

Clukey, E. C. and Phillips, R. (2002). Centrifuge model tests to verify suction caisson capacities for taut and semi-taut legged mooring systems. *Proceedings, International Conference on Deepwater Offshore Technology*.

Dangayach, S. 2004. Reliability Analysis of Mooring System for Spar. *M. S. Thesis, University of Texas at Austin:* 84 pp.

Ding, Y., Kim, M., Chen, X. and Zhang, J. 2003. Coupled Analysis of Floating Production System. *Proc. Intern. Symp. on Deepwater Mooring Systems, Concepts, Design, Analysis, and Materials, Houston, Texas*: 152-167.

El-Sherbiny, Rami M. (2005), "Performance of Suction Caisson Anchors in Normally Consolidated Clay", Ph.D. dissertation, University of Texas, Austin, August.

Gilbert, R. B. and Murff, J. D. (2001), "Identifying Uncertainties in the Design of Suction Caisson Foundations," *Proceedings,* International Conference on Geotechnical, Geological and Geophysical Properties of Deepwater Sediments Honoring Wayne A. Dunlap, OTRC, Houston, Texas, 231-242.

Gilbert, R. B. (2003), "Reliability-Based Design as a Decision-Making Tool," Proceedings, International Workshop on Limit State Design in Geotechnical Engineering Practice, Phoon, Honjo and Gilbert (eds.), Cambridge, Massachusetts.

Gilbert, R. B., Najjar, S. S., Choi, Y. J. (2005). Incorporating lower-bound capacities into LRFD codes for pile foundations. *Proceedings, GeoFrontiers Conference,* ASCE, inpress.
Goodwin, P., Ahilan, R. V., Kavanagh, K. and Connaire, A. 2000. Integrated Mooring and Riser Design: Target Reliabilities and Safety Factors. *Proc. of OMAE*: 185-792.
Hamilton, J. M. and Murff, J. D. 1992. Selection of LRFD Resistance Factors for Pile Foundation Design. *Proc. of Structural Congress '92,* ASCE, San Antonio, Texas: 788-795.
Horsnell, M. R. and Toolan, F. E. .1996. Risk of Foundation Failure of Offshore Jacket Piles. *Proc. of Offshore Tech. Conf.*, OTC 7997: 381-392.
House, A. R., and Randolph, M. F. (2001). Installation and pullout capacity of stiffened suction caissons in cohesive sediments. *Proceedings, 11th International Offshore and Polar Engineering Conference.*
Jeanjean, P. Znidarcic, D., Phillips, R. Ko, H.Y., Pfister, S., Cinicioglu, O. and Schroeder, K. (2006), "Centrtifuge Testing on Suction Anshors: Double-Wall, Overconsolidated Clay, and Layered Soil Profile," *Proceedings, Offshore Technology Conference,* OTC 18007.
Luke, A. M., Rauch, A. F., Olson, R. E., and Mecham, E. C. (2003). Behavior of suction caissons measured in laboratory pullout tests. *Proceedings of the International Conference on Offshore Mechanics and Arctic Engineering*, OMAE, pages-9.
Murff, J. D. and Hamilton, J. M. (1993). P-Ultimate for undrained analysis of laterally loaded piles. *Journal of Geotechnical Engineering*, ASCE, Vol. 119, No. 1, 91-107.
Najjar, S. S. (2005), "Importance of Lower-Bound Capacities in Geotechnical Reliability Assessments," *Ph.D. Dissertation, The University of Texas at Austin*: 317 pp.
Neubecker, S. R. and Randolph, M. F. 1995. Performance of Embedded Anchor Chains and Consequences for Anchor Design. *Proc. Offshore Technology Conf., OTC 7712, Houston, Texas:* 191-200.
Randolph, M. F., and House, A. R. (2002). Analysis of suction caisson capacity in clay. *Proceedings, Offshore Technology Conference*, OTC 14236.
Ronold, K. O. 1990. Reliability Analysis of Tension Pile. *Journal of Geotech. Engineering, Vol. 116, No. 5:* 760-773.
Smith, G. L. and Gilbert, R. B. (2001), "A Simplified Model of Spatial Variability to Evaluate Effects of Spatial Averaging on Foundation Capacity," *Proceedings*, International Conference on Structural Safety and Reliability, Huntington Beach, California.
Tang, W. H. 1990. Performance Reliability of Offshore Piles. *Proc. of Offshore Tech. Conf.*, OTC 6379: 299-308.
Tang, W. H. and Gilbert, R. B. 1993. Case Study of Offshore Pile System Reliability. *Proc. of Offshore Tech. Conf.,* OTC 7196: 677-686.
Watson, P. G., Suemasa, N., and Randolph, M. F. (2000). Evaluating Undrained Shear Strength Using the Vane Shear Apparatus. *Proceedings, 10th International Offshore and Polar Engineering Conference,* 485-493.
Winterstein, S. R. and Kumar, S. 1995. Reliability of Floating Structures: Extreme Response and Load Factor Design, *Proc. Offshore Technology Conf., OTC 7758, Houston, Texas:* 569-578.

Appendix A

Description of Geotechnical Database Design

Database Features

The geotechnical data are stored in Microsoft Access®, which is a relational database. In general, data in the Access® database can be queried, sorted, placed in a report, or exported for analysis and visualization. Once exported, data can be analyzed with a spreadsheet program or modeled with modeling or visualization software. The database contains Tables, Queries, Forms, and a Module. These features are described below.

<u>Tables—Data Storage and Entry</u>

The data are organized in Tables. An example of a Table with Unconsolidated Undrained (UU) triaxial data is shown below in Fig. A.1.

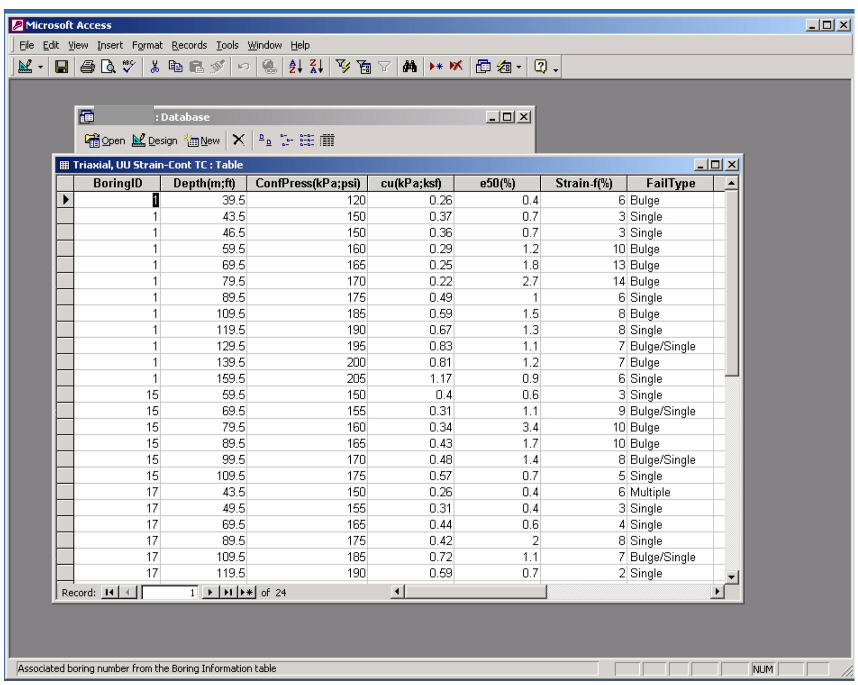

BoringID	Depth(m;ft)	ConfPress(kPa;psi)	cu(kPa;ksf)	e50(%)	Strain-f(%)	FailType
1	39.5	120	0.26	0.4	6	Bulge
1	43.5	150	0.37	0.7	3	Single
1	46.5	150	0.36	0.7	3	Single
1	59.5	160	0.29	1.2	10	Bulge
1	69.5	165	0.25	1.8	13	Bulge
1	79.5	170	0.22	2.7	14	Bulge
1	89.5	175	0.49	1	6	Single
1	109.5	185	0.59	1.5	8	Bulge
1	119.5	190	0.67	1.3	8	Single
1	129.5	195	0.83	1.1	7	Bulge/Single
1	139.5	200	0.81	1.2	7	Bulge
1	159.5	205	1.17	0.9	6	Single
15	59.5	150	0.4	0.6	3	Single
15	69.5	155	0.31	1.1	9	Bulge/Single
15	79.5	160	0.34	3.4	10	Bulge
15	89.5	165	0.43	1.7	10	Bulge
15	99.5	170	0.48	1.4	8	Bulge/Single
15	109.5	175	0.57	0.7	5	Single
17	43.5	150	0.26	0.4	6	Multiple
17	49.5	155	0.31	0.4	3	Single
17	69.5	165	0.44	0.6	4	Single
17	89.5	175	0.42	2	8	Single
17	109.5	185	0.72	1.1	7	Bulge/Single
17	119.5	190	0.59	0.7	2	Single

Fig. A.1. A table in the database

Data can be entered directly into a Table. Data can also be modified and deleted in Tables. To modify data, highlight the incorrect entry and type a new one in its place. Records can be deleted by highlighting the entire record(s); Access® will prompt you "do you really want to delete" the selected text. Access® will not allow the deletion of multiple entries, only multiple records; entry deletions can only be done one at a time.

Data can also be pasted into a Table from a spreadsheet (a cut and paste operation). Entering data from a spreadsheet involves highlighting the data in the spreadsheet, copying it (to the clipboard), selecting the last record in the Access® Table, and choosing "Paste Append" from "Edit." In pasting operations, it is necessary that the fields line up properly.

Queries—Data Manipulation

Queries are used to narrow down the data or to select certain types of information, such as the undrained shear strength measured at borings within certain coordinates or at certain depths. An example of a Query to call up all samples with moisture content, plastic limit and liquid limit, as well as calculate the plasticity and liquid indices is shown below in Fig. A.2. The example result of a query, which has been pasted into Excel® for plotting, is shown on Fig. A.3.

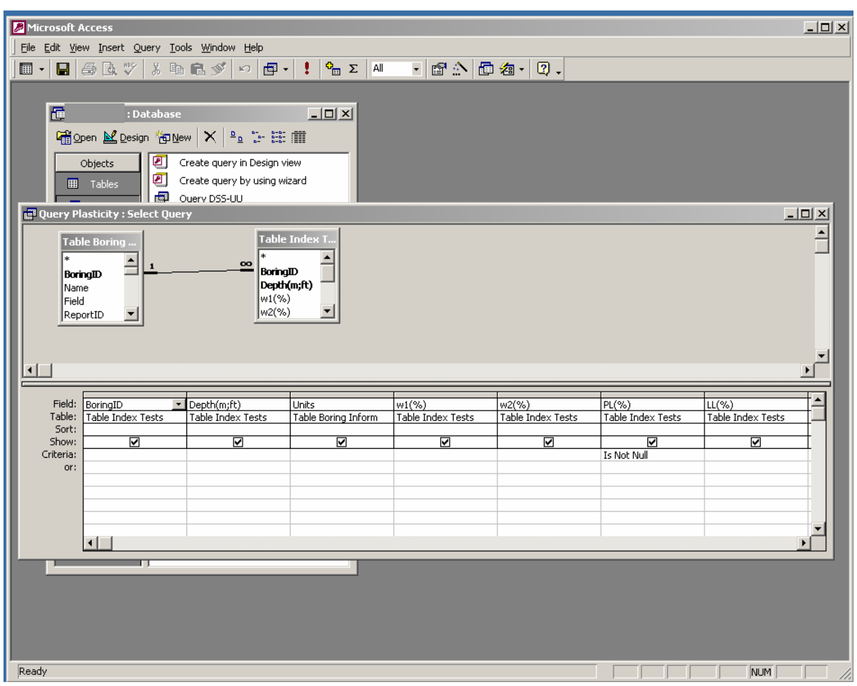

Fig. A.2. A query in Design View. A query viewed in Datasheet View looks like a table.

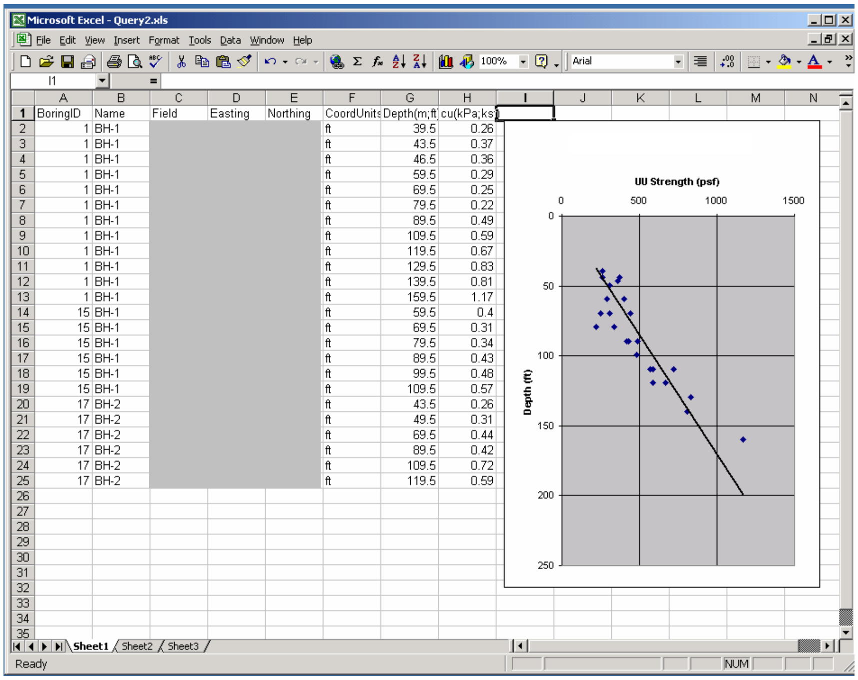

BoringID	Name	Field	Easting	Northing	CoordUnits	Depth(m;ft	cu(kPa;ks
1	BH-1				ft	39.5	0.26
1	BH-1				ft	43.5	0.37
1	BH-1				ft	46.5	0.36
1	BH-1				ft	59.5	0.29
1	BH-1				ft	69.5	0.25
1	BH-1				ft	79.5	0.22
1	BH-1				ft	89.5	0.49
1	BH-1				ft	109.5	0.59
1	BH-1				ft	119.5	0.67
1	BH-1				ft	129.5	0.83
1	BH-1				ft	139.5	0.81
1	BH-1				ft	159.5	1.17
15	BH-1				ft	59.5	0.4
15	BH-1				ft	69.5	0.31
15	BH-1				ft	79.5	0.34
15	BH-1				ft	89.5	0.43
15	BH-1				ft	99.5	0.48
15	BH-1				ft	109.5	0.57
17	BH-2				ft	43.5	0.26
17	BH-2				ft	49.5	0.31
17	BH-2				ft	69.5	0.44
17	BH-2				ft	89.5	0.42
17	BH-2				ft	109.5	0.72
17	BH-2				ft	119.5	0.59

Fig. A.3. Data from the Query is pasted into Excel to be plotted and analyzed.

Queries can get information from Tables or other Queries. For example, the data can be further defined by querying a Query. The data can also be modified through Queries. For example, if an error is detected during a Query it can be corrected in the Query and will be reflected in the Table and other Queries that contain that data.

Query design is generally a point and click operation with logical operators used to narrow down a selection. Access® provides an "expression builder" when the user right clicks in the "criteria" field of the Query design screen. For non-routine Queries, the on-line help is useful.

Forms—Automation

Forms are used to make using the database more convenient. For example, they may be used to automate common processes, or display data from a Table in a way more pleasing to the eye. A Form is based upon one or more Tables or Queries. The data in a Form may be displayed in datasheet mode (looks like a Table) or in standard form mode. Standard form mode shows only one record at a time. You can toggle between the two views by right-clicking the title bar of the Form and selecting the other view from the menu. In the standard form mode, you may use "controls," which include text boxes, image frames, buttons, and menus. Forms allow the user to invoke certain actions (Macros or Modules) by performing certain actions (for example, clicking a button or modifying a text box). Data may be entered or modified directly in a Form. While a Form is based on a Table/Query, its format is not automatically updated. For example, if you created a new field in a Table, that field would not automatically appear on the old Form. A standard form view of DSS data with an accompanying Form showing stress-strain response and stress path is shown below.

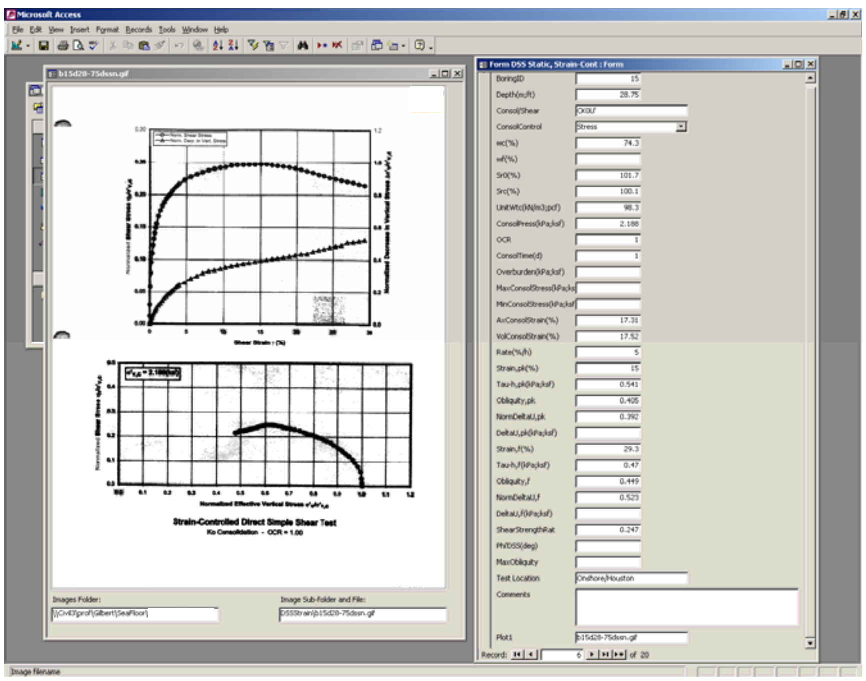

Fig. A.4. An image form and a record in Form View.

Modules—Programming Forms

Microsoft Access® uses Visual Basic to perform macros, including actions associated with Forms. Much of the time, the code will be contained in the design of the Form itself. When actions involve more than one Form, a Module separate from all the Forms is often used. Although the database user will probably never look at the Module, and it contains no data from the database, it is important that it exists and functions so features associated with Forms will function properly**.**

Database Structure

The database allows data entry and manipulation in three ways: Tables, Queries, and Forms. Tables contain raw data. Queries may filter, calculate, or join data from Tables or other Queries. Forms may display the data from a Table or Query in a more meaningful way and may employ Modules to do it. In this section, the Tables, Queries, Forms, and Modules included with this database are summarized.

Data Tables

The data are organized into 26 Tables. A list of these Tables and a description of their organization is presented below in Table A.1. The data contained in each Table is generally intuitive. Most Tables contain data from a certain test. Shear strength tests with several parameters each have a unique Table. Tests with many inputs or outputs have a unique Table. Shear strength tests with only 1 or 2 parameters appear together in the *Simple Strength Tests* Table. Generally, other tests with only a boring number, a sample/test depth, and one output are grouped in the *Index Tests* Table. Images that apply to a group of tests or the entire boring are recorded in the *Images Advanced Tests*, *Images Summary*, and *Images Xray* Tables: Note that Tables only contain the image file names and cannot be used to view the images; to view the images, the associated Form must be used.

Table A.1. Summary of Database Tables

Table Name	Type of Data
Abbreviations	A list of abbreviations commonly used in the database
Database Comments	A few comments about the creation and maintenance of the database
Info	Information related to Form Image
Boring Information	Name, Boring Type, Dates, Sampling Method, Driller, Engineer, Water Depth, Boring/CPT Log Image, Units.
Location Data	Geographic Coordinates, Projected Coordinates, Geographic Data
Boring Log	Soil Type, Physical Description
Cone Penetration Test	CPT Tip Resistance, Excess Pore Pressure, and Friction Ratio.
Consolidation	Soil Compressibility Data: Compression Index, Recompression Index, Coefficient of Consolidation, Individual Test Plots
Design Profile	Profiles of Shear Strength, Pile Friction and Bearing Parameters, and Submerged Unit Weight, recommended by the Engineer
DSS Tables	Consolidation control, Shearing control, Strain rate, Shear Stress, Pore Pressure, Individual Test Plots
Grain Size	Percent smaller than standard sieve and hydrometer sizes from #4 to 1 μm, Individual Test Plot
Hydraulic Conductivity	Permeant, Unit Weight, Consolidation Time, Confining Stress, Hydraulic Gradient, Interpreted Hydraulic Conductivity
Index Tests	Moisture Content, Unit Weight, Carbonate Content, Plastic Limit, Liquid Limit, Specific Gravity of Solids
Piezoprobe	Hydrostatic Pressure, Peak Pore Pressure, Excess Pore Pressure, Interpreted Hydraulic Conductivity, Individual Test Plots
Resonant Column	Consolidation Pressures, Shear Modula, Fitting Parameters, Individual Test Plots
Simple Strength Tests	Minivane, Torvane, Dolphin and Halibut Field Vanes (including Individual Test Plots), Pocket Penetrometer
Triaxial Tables	Consolidation Pressure and Strain, Rate of Strain, Shear and Mean stress, Pore Pressures, Individual Test Plots
Images Advanced Tests	Images of summaries of groups of tests from the Advanced Testing Program done by the Engineer: Boring, Description, Associated Test Type, Applicable Depth Range
Images Summary	Images concerning the boring in general: Boring, Description
Images Xray	Xrays of saved tube and quart samples: Boring, Depth

The data in the soil boring investigations are usually recorded in their original units, and a field in the *Boring Information* Table is used to indicate the type (English or Metric) of units for the data. Where the units have been changed (e.g. from tons per square foot to kips per square foot), there is an accompanying note stating what the original units were. The *Boring Information* Table is the central Table of the database; most Tables are related to it in some way.

Boring Information

Primary information for each boring is stored in the Boring Information Table. This is unique information for each boring and requires one record per boring. This information includes a boring identification number, the area or field where it was drilled, report numbers, dates, engineer, driller, water depth, boring method, sampling method, final depth, images of the boring/CPT logs, and type of units used (English or Metric). The numerical location data—geographic coordinates and projected coordinates (e.g. UTM coordinates) and their respective geographic data—are contained in the Location Data Table. Other applicable images (such as design profiles, plasticity profiles, and location map) may be found in the Images Summary Table.

Index Properties

Two Tables are used to store records based on index property tests. These data include Atterberg limits, weight-volume information, and grain size. Plastic and liquid limit test results at a given depth for each boring are listed in the Index Tests Table. This Table also includes weight-volume information, such as water content, unit weight, carbonate content, and specific gravity of solids. The Grain Size Table stores the measured percent passing the United States Standard (USS) sieve numbers 4 and 200 and the ASTM standard hydrometer sizes 5 μm and 1 μm. The values reported as fines, or silts and clays are defined as the percent passing the number USS 200 sieve or grain sizes less than 75 μm. Both Tables include Boring ID and Depth to uniquely identify each test and to link it to the proper boring in the Boring Information Table. Summary plots of these tests may be found in the Images Summary Table.

Laboratory Engineering Properties

Lab-measured engineering properties are stored in Tables according to the test type. The data include consolidation, direct simple shear (DSS), hydraulic conductivity, minivane, torvane, pocket penetrometer, resonant column, and triaxial measurements. Each test is identified by depth and boring number from the Boring Information Table.

Many tests include an image file in the Table. Summary images for tests that were part of the Advanced Testing Program (Cyclic DSS and Triaxial tests, Stress and Strain Controlled Triaxial tests--not including UU Tests, Stress Controlled DSS Tests, Resonant Column Tests, and some Strain Controlled DSS Tests) may be found in the Images Advanced Tests Table. These may include plots such as strain vs. shear stress and log of time, or cyclic stress ratio vs. number of cycles. Saved sample X-rays are found on the Images Xray Table. Other summary images not applying exclusively to the Advanced Testing Program may be found in the Images Summary Table.

So far, the database contains data from undrained strength tests only. Minivane, Torvane, and Pocket Penetrometer results are given in the Simple Strength Tests Table. Complex test results are given in the DSS, Triaxial, and Resonant Column Tables. Each of them contains index properties measured during or after the test (the initial index properties are recorded in the Index Properties Table). They also contain consolidation and rate of strain data.

There are three Tables for different direct simple shear tests. All of them include image files. The DSS Static, Strain-Cont Table contains strains, stresses, and pore pressures at peak horizontal shear stress and at high strain. The DSS Static, Stress-Cont Table contains data pertinent to a creep test, such as loading stress and time increments, applied stress, and a few time-strain pairs. The DSS Cyclic, Stress-Cont Table contains data for cyclic shear stress controlled tests. The data include ambient shear strain, average cyclic shear stress, cyclic shear stress amplitude, and some pairs of number of cycles vs. average shear strain and vs. cyclic shear strain.

There are five Tables for different triaxial shear tests. All of them include image files. The Triaxial, UU Strain-Cont TC Table contains data from unconsolidated, undrained, strain-controlled triaxial compression tests, including confining pressure, undrained shear strength, failure strain, rate of strain, and mode of failure. The Triaxial, Strain-Cont TC and Triaxial, Strain-Cont TE Tables contain data for consolidated, undrained, strain-controlled compression and extension tests, respectively. The Tables record K0 where applicable, as well as strain rate, mean and shear stress, principal stress ratio, pore pressures, and mode of failure. Consolidated undrained triaxial compression creep test results are recorded in the Triaxial, Stress-Cont TC Table, and loading stress and time increments are given, as well as shear strain vs. time pairs and a reference undrained shear strength. The Triaxial, Stress-Cont Cyclic Table contains data from consolidated undrained stress-controlled cyclic triaxial tests. Frequency and amplitude of the load are recorded, along with vertical and horizontal consolidation pressures, and some pairs of number of cycles vs. average shear strain and vs. cyclic shear strain.

The Resonant Column Table contains consolidation pressure and maximum shear modulus for each stage, as well as empirical parameters for fitting maximum shear modulus vs. consolidation pressure, as well as image files.

The Consolidation Table stores the maximum previous consolidation pressure, constrained modulus for each increment, coefficient of consolidation, and the overconsolidation ratio, as well as image files.

The Hydraulic Conductivity Table contains test parameters before, during, and after the test. These data include void ratio, consolidation pressure, hydraulic gradient, permeant, specimen orientation (horizontal vs. vertical permeability), water content, and hydraulic conductivity. There are no individual test plots.

Field Engineering Properties

Field measured soil properties are recorded in three Tables, which uniquely identify each data point by its Boring identification number and depth. These Tables are *Cone Penetration Test*, *Piezoprobe*, and *Simple Strength Tests*.

The *Cone Penetration Test* Table stores point data entered for continuous CPT data. The data consist of cone resistance, pore water pressure, and friction ratio as a function of depth. Entered point data vary from 0.5 to 2 feet (0.2 to 0.5 meters) of depth, depending on the resolution required to reflect the variability of the cone measurements. The image of the CPT log may be found on the *Boring Information* Table.

The *Piezoprobe* Table contains pore pressure data measured in the field, including hydrostatic pressure, peak pore pressure, estimated pore pressure, excess pore pressure, and hydraulic conductivity. Plots are included.

Dolphin and Halibut field vane test results are found in the *Simple Strength Tests* Table. The information includes the blade size and the measured in-situ and remolded shear strengths. Images are included.

<u>Design Information</u>

Design information is recorded in two Tables. The *Boring Log* Table stores the soil descriptions as interpreted from the boring logs by the engineers. This Table, which is linked to the *Boring Information* Table, includes the depth intervals and description of each soil stratum. The description generally gives information about density, gradation, strength, and color; for example "Gray medium dense fine sand' or "Stiff gray clay". An image of the boring log may be found on the *Boring Information* Table.

The *Design Profile* Table includes the design parameters for axial and lateral pile capacity as interpreted by the engineers based on measured values. These data include design undrained shear strength, design friction angle, and submerged unit weight, the strain at 50 percent deviator stress in a triaxial undrained test, and subgrade modulus. Design profile plots may be found in the *Images Summary* Table.

<u>Supplemental Information</u>

Some supplemental information is recorded in two Tables. The *Abbreviations* Table gives a list of abbreviations used elsewhere in the database. The *Database Comments*

Table gives a brief description of how the database was designed. The *Info* Table provides the Images directory path to the *Image* Form.

Queries

Six Queries have been created for this database. They are listed below in Table A.2 along with a summary of the information that they provide. Typical Queries for this database involve one or two Tables. When two Tables are queried, one of them is usually the *Boring Information* Table, as this Table is linked to the other data Tables.

Table A.2. Summary of Database Queries

Query Name	Type of Data
DSS-UU	Boring, Depth, UU Peak Shear Strength, DSS Peak Shear Stress; demonstrates renaming a field and how to use the Test Depths union query
Map Grid	Boring ID, Name, Field, Projected Coordinates, Water Depth, Boring Depth, Units
Plasticity	Boring, Depth, Moisture Content, Plastic Limit, Liquid Limit, Plasticity Index, Liquidity Index, Units; demonstrates calculations in a query
Su Profile	Start and End Depths, Start and End Undrained Shear Strengths, Units
Sub Unit Weight	Boring, Depth, Measured Submerged Unit Weight, Units
Test Depths	Union Query of all Boring/Depth combinations from all test Tables

Forms

The database includes 18 Forms. Each of them is based on one Table. They are used to allow viewing of images stored in the database. A list of Tables and their associated Forms is given below in Table A.3. For Tables that hold no image data, there is no associated Form. The *Image* Form will never be used by itself, except for database installation. However, it is the Form that opens as a result of an event (a double-click) in another Form and displays the correct image.

To view an image is simple: Just double-click on the name of the file. A new *Image* Form will open and the image will be displayed. The path to the Images directory is shown below and to the left of the image, while the path and filename relative to that directory is shown below and to the right of the image. The file name appears in the title bar. Multiple *Image* Forms may be open at once. Each one can be closed separately.

Table A.3. Tables and their Associated Forms

Table Name	Associated Form Name
Abbreviations	--
Boring Information	Boring Information
Boring Log	--
Cone Penetration Test	--
Consolidation	Consolidation
Database Comments	--
Design Profile	--
DSS Cyclic, Stress-Cont	DSS Cyclic, Stress-Cont
DSS Static, Strain-Cont	DSS Static, Strain-Cont
DSS Static, Stress-Cont	DSS Static, Stress-Cont
Grain Size	Grain Size
Hydraulic Conductivity	--
Images Advanced Tests	Images Advanced Tests
Images Summary	Images Summary
Images Xray	Images Xray
Index Tests	--
Info	Image
Location Data	--
Piezoprobe	Piezoprobe
Resonant Column	Resonant Column
Simple Strength Tests	Simple Strength Tests
Triaxial, Strain-Cont TC	Triaxial, Strain-Cont TC
Triaxial, Strain-Cont TE	Triaxial, Strain-Cont TE
Triaxial, Stress-Cont Cyclic	Triaxial, Stress-Cont Cyclic
Triaxial, Stress-Cont TC	Triaxial, Stress-Cont TC
Triaxial, UU Strain-Cont TC	Triaxial, UU Strain-Cont TC

Modules

The database includes one Module called *basPublic*. It is used by all of the Forms to open a new *Image* Form and to maintain the *Image* Forms while they are open.